frontiers in Materials

TYPE Original Research
PUBLISHED 21 April 2026
DOI 10.3389/fmats.2026.1755011

OPEN ACCESS

EDITED BY
Svetlana Tretsiakova,
Ulster University, United Kingdom

REVIEWED BY
Ayub Elahi,
University of Engineering and Technology, Taxila, Pakistan
Dayou Luo,
Iowa State University, United States

*CORRESPONDENCE
Amani Abdallah Hepautwa,
hepautwaamani@gmail.com
Yusufu Abeid Chande Jande,
yusufu.jande@nm-aist.ac.tz

RECEIVED 26 November 2025
REVISED 06 March 2026
ACCEPTED 09 March 2026
PUBLISHED 21 April 2026

CITATION
Hepautwa AA, Hilonga A, Mrosso R, Alfredy T, Lesafi F and Chande Jande YA (2026) Mechanical, durability, and thermal performance of concrete incorporating coffee biochar and raw and calcined montmorillonite. *Front. Mater.* 13:1755011. doi: 10.3389/fmats.2026.1755011

Mechanical, durability, and thermal performance of concrete incorporating coffee biochar and raw and calcined montmorillonite

Amani Abdallah Hepautwa [1,2]*, Askwar Hilonga[1], Register Mrosso[1], Tusekile Alfredy[1], Fina Lesafi[1] and Yusufu Abeid Chande Jande[1,3]*

[1]Department of Materials and Energy Sciences and Engineering, Nelson Mandela African Institution of Science and Technology, Arusha, Tanzania, [2]Department of Civil and Irrigation Engineering, Mwalimu Julius K. Nyerere University of Agriculture and Technology, Musoma, Tanzania, [3]Water Infrastructure and Sustainable Energy Futures (WISE-Futures) African Centre of Excellence, The Nelson Mandela African Institution of Science and Technology, Arusha, Tanzania

Introduction: Montmorillonite is a natural aluminosilicate clay with potential as a supplementary cementitious material, although its reactivity in the raw state is limited. This study investigates the effect of raw and calcined montmorillonite on the performance of concrete incorporating 15% pyrolyzed coffee grounds (PCG) at 350 °C.
Methods: Montmorillonite calcined at 400, 600, and 800 °C replaced cement at levels of 5%–20%. Mechanical and durability properties were evaluated under acidic, saline, and thermal exposure conditions. Microstructural characterization was conducted using FTIR, XRD, and SEM, and statistical validation was performed using two-way ANOVA.
Results: Calcination enhanced montmorillonite reactivity through amorphization and pozzolanic reactions, resulting in improved pore refinement and matrix densification. Specimens with calcined montmorillonite at 600 °C–800 °C showed superior strength and durability performance.
Discussion: The combined use of calcined montmorillonite and 15% PCG biochar at 350 °C provides a sustainable approach for improving concrete performance.

KEYWORDS
coffee biochar, hardness behavior, hazardous environment, mechanical behavior, montmorillonite

1 Introduction

Concrete remains the backbone of modern infrastructure because of its high compressive strength, adaptability, and cost-effectiveness. However, its inherent limitations—low tensile and flexural strength, susceptibility to cracking, and reduced durability in aggressive environments—restrict its performance in demanding conditions. More critically, the production of Portland cement, the principal binder in concrete, is highly energy intensive and emits approximately 0.8–0.9 tones of CO_2 per tonne of clinker, contributing nearly 8% of global CO_2 emissions. With rapid urbanization and infrastructure expansion, the

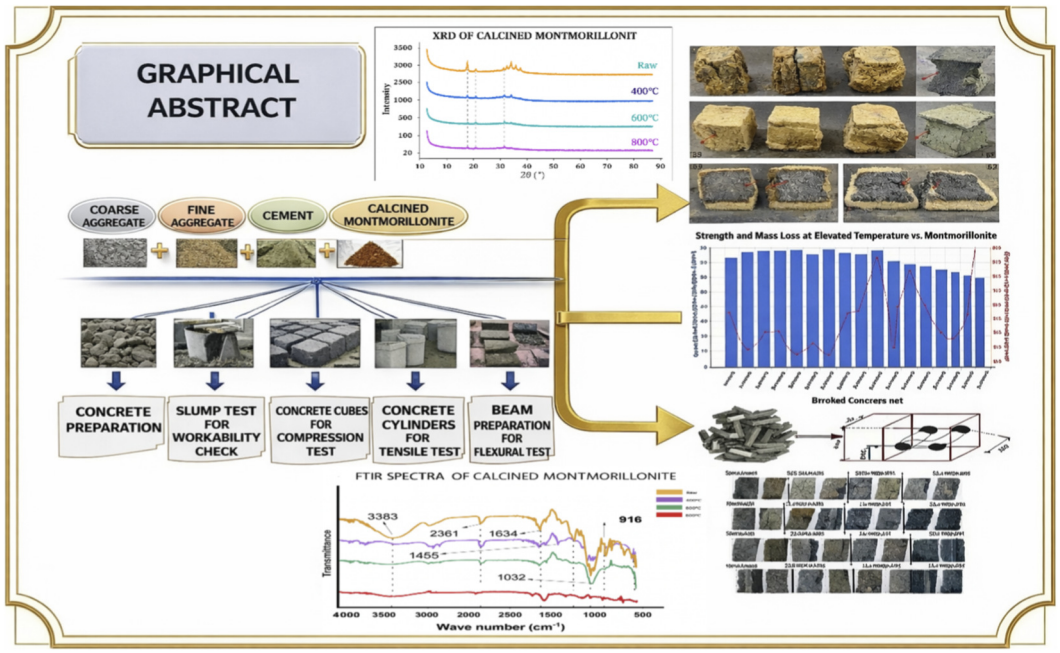

GRAPHICAL ABSTRACT

urgency to adopt sustainable supplementary cementitious materials (SCMs) that reduce cement consumption while maintaining or improving performance has never been greater (Langaroudi and Mohammadi, 2018; Lei et al., 2021; Rashid et al., 2024; Rashidi et al., 2024; Shamsa et al., 2022; Haigh et al., 2024; Macías-Párraga et al., 2025; Eliche-Quesada et al., 2021; Gomes et al., 2024).

Among the wide range of SCMs investigated—such as fly ash, silica fume, rice husk ash, and metakaolin—montmorillonite (MMT) has attracted increasing attention due to its abundance, low cost, and high silica (SiO_2) and alumina (Al_2O_3) contents. Raw MMT exhibits moderate pozzolanic activity and contributes a filler effect, but its crystalline structure restricts reactivity, limiting its effectiveness. For instance, (Langaroudi and Mohammadi, 2018), reported that incorporating uncalcined montmorillonite at 10%–20% replacement slightly improved compressive strength at early ages but reduced long-term performance due to unreacted crystalline phases. Similarly, (Langaroudi and Mohammadi, 2018) found only a 5%–7% improvement in strength with raw montmorillonite, compared to 15%–20% gains from metakaolin or silica fume under comparable conditions. These findings underscore the need to activate MMT before it can rival conventional SCMs (Latifi et al., 2018; Madirisha et al., 2019; Onyelowe et al., 2019; Marangu, 2020; Attah et al., 2023).

Thermal activation (calcination) is a proven method to enhance the reactivity of clay-based materials. Calcination between 500 °C and 800 °C disrupts the crystalline lattice of montmorillonite, removes hydroxyl groups, and increases the content of amorphous silica and alumina phases—key drivers of pozzolanic reactions (Langaroudi and Mohammadi, 2018; Lei et al., 2021; Rashid et al., 2024; Abdalla et al., 2023). Demonstrated that calcined clay improved mortar surface hardness by 25%, while (Shamsa et al., 2022; Ahmed, 2024; DuchesneJ, 2021; Fode et al., 2023) observed up to 30% reduction in chloride permeability in mortars containing calcined montmorillonite. More recently, (Langaroudi and Mohammadi, 2018; Lei et al., 2021; Rashid et al., 2024; Rashidi et al., 2024; Wang and Zhang, 2025; Wang et al., 2019; Abdalla et al., 2023), reported that calcination at 700 °C–800 °C enhanced C–S–H gel formation and refined pore structure, leading to improved compressive strength and durability (Langaroudi and Mohammadi, 2018; Lei et al., 2021; Rashid et al., 2024; Rashidi et al., 2024; Shamsa et al., 2022). These results confirm that properly activated MMT can perform comparably to high-grade pozzolans like metakaolin (Kaundal et al., 2025; Gu et al., 2024; Laidani et al., 2020; Liu et al., 2020).

Despite these promising results, most previous research has been limited in scope. Some studies evaluated only mechanical strength, while others focused on a single durability index such as chloride resistance. Few have systematically examined the combined effects of raw and calcined MMT under multiple hazardous exposures, including acidic, saline, and elevated temperature conditions. For example, (Lei et al., 2021) studied bentonite-modified mortars in HCl solutions but did not compare the effects of different calcination temperatures. Similarly, (Langaroudi and Mohammadi, 2018; Lei et al., 2021; Rashid et al., 2024; Abdalla et al., 2023), investigated chloride

Abbreviations: MMT, Montmorillonite; PCG, Pyrolyzed coffee grounds; OPC, Ordinary Portland cement; SCM, Supplementary cementitious material; C–S–H, Calcium silicate hydrate; C–A–S–H, Calcium aluminate silicate hydrate; Ca(OH)2, Calcium hydroxide; ITZ, Interfacial transition zone; w/c, Water-to-cement ratio; FTIR, Fourier transform infrared spectroscopy; XRD, X-ray diffraction; SEM, Scanning electron microscopy; ANOVA, Analysis of variance; SAI, Strength activity index.

penetration resistance of MMT concretes but did not incorporate mechanical testing or microstructural analysis. Furthermore, while studies on fly ash and metakaolin often apply statistical models to validate factor interactions, similar approaches are rarely reported for MMT. This leaves an important research gap in fully understanding how calcination temperature and replacement levels interact to influence both strength and durability.

The present study addresses these gaps by comprehensively evaluating the performance of concrete composites incorporating raw montmorillonite (0 °C) and calcined montmorillonite (400, 600, and 800 °C) at replacement levels of 5%, 10%, 15%, and 20%. Mechanical properties assessed include compressive, tensile, flexural strength, and Vickers hardness, while durability was examined through mass loss in 5% HCl, 5% HNO_3, and 10% NaCl solutions, residual strength after exposure to elevated temperature (200 °C), and corrosion potential of embedded steel bars. In addition, advanced characterization techniques (FTIR, XRD, SEM, DSC) were used to establish microstructural links to performance outcomes.

A key novelty of this study is the application of two-way ANOVA alongside pairwise statistical comparisons to quantify the independent and interactive effects of calcination temperature and replacement percentage. This approach provides a more robust evaluation than previous studies, which often report only mean values without statistical validation. For example, while (Langaroudi and Mohammadi, 2018; Lei et al., 2021; Rashid et al., 2024; Rashidi et al., 2024; Shamsa et al., 2022; Wang and Zhang, 2025; Wang et al., 2019; Abdalla et al., 2023). Confirmed improvements qualitatively, they did not explicitly test the significance of factor interactions, leaving uncertainties in optimizing dosage and calcination conditions. By contrast, this work demonstrates that calcination temperature, replacement dosage, and their interactions are statistically significant ($p < 0.05$) across bulk density, strength, and durability outcomes.

From a sustainability perspective, the benefits of incorporating calcined MMT are twofold. First, replacing 15%–20% of cement with MMT calcined at 600 °C–800 °C can reduce cement consumption, thereby lowering CO_2 emissions associated with clinker production. Second, the improved durability—particularly the 85% reduction in mass loss under nitric acid exposure and the >30% increase in Vickers hardness—translates into longer service life and reduced maintenance needs, further lowering the environmental footprint of concrete structures. When compared to other SCMs such as rice husk ash (RHA) or fly ash, calcined MMT shows comparable performance improvements but with the added advantage of local availability in regions where volcanic ash or industrial by-products are scarce.

Generally, this study aims to provide a holistic evaluation of montmorillonite as a sustainable SCM by combining microstructural characterization, mechanical and durability testing, and statistical validation. By comparing raw and thermally activated forms across multiple hazardous environments, it establishes the optimal replacement levels and calcination temperatures for maximizing both performance and sustainability. Ultimately, the findings position calcined montmorillonite as a viable alternative SCM that not only reduces cement dependency but also enhances the resilience of concrete in aggressive service conditions—thereby contributing to global efforts in sustainable construction.

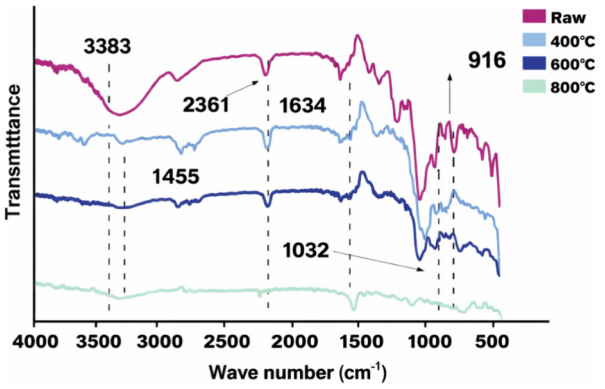

FIGURE 1
FTIR analysis.

2 Materials preparation

The raw montmorillonite used in this study was sourced from Tanga, Tanzania. Upon collection, the raw montmorillonite was subjected to a grinding process using a laboratory ball mill to achieve a uniform particle size. After grinding, the material was sieved through a number 325 sieve to remove larger particles and ensure a fine powder suitable for incorporation into cement composites.

Following the grinding and sieving processes, the montmorillonite was calcined at varying temperatures to enhance its pozzolanic reactivity. The calcination was performed at 400 °C, 600 °C, and 800 °C for a duration of 3 h. These temperatures were selected based on previous research indicating optimal dihydroxylation and reactivity characteristics for montmorillonite. The resulting calcined montmorillonite was then allowed to cool and stored in airtight containers to prevent moisture absorption.

The mortar specimens used in this study have four components cement, sand, water, and montmorillonite. The ordinary Portland cement (OPC) of CEM I 32.5 R was used for the preparation of mortar at a plane and different substitutions of raw and calcined montmorillonite as shown in Figure 1. The aggregate used is fine aggregate as the ASTM standard presented in Table 2. The water used is the distilled water supplied by the Tanga cement PLC., where this study was conducted.

The chemical composition of both Raw and calcined montmorillonite was analyzed using X-ray fluorescence (XRF) to confirm that the oxide composition of SiO_2, Al_2O_3, and Fe_2O_3 exceeded 70%, in line with the minimum requirements set by ASTM C618 for pozzolanic materials.

2.1 Gradation of used fine aggregate

Raw montmorillonite was obtained from a natural clay deposit located in Arusha, Tanzania. This region is known for its rich mineral resources, including clays with high montmorillonite content suitable for use in cementitious materials. Upon extraction, the raw montmorillonite was subjected to preliminary preparation to ensure uniform particle size and consistency for further processing. The material was first dried under ambient laboratory conditions to remove any free moisture content, followed by grinding using

TABLE 1 Gradation Of Used Fine Aggregate.

Sieve size (mm)	Percentage passing (upper limit)	Percentage passing (used sand)	Percentage passing (lower limit)
1.18	100	100	100
0.85	98.2	98.5	97.8
0.60	97.5	97.9	94.8
0.425	90.1	86.6	67.6
0.30	70.3	65.3	44.7
0.212	44.6	37.5	24.9
0.15	10.1	7.4	3.4

a laboratory ball mill machine to achieve fine powder suitable for cementitious applications. After grinding, the powder was passed through a No. 325 sieve (45 microns opening) to ensure that the particles met the standard fineness required for pozzolanic materials. Any residue retained on the sieve was weighed and recorded, as detailed in Table 1, in order to assess the milling efficiency and particle size distribution.

Following the grinding and sieving process, calcination of the montmorillonite samples was carried out to enhance their pozzolanic reactivity. The raw powder was thermally treated in a muffle furnace at three selected temperatures: 400 °C, 600 °C, and 800 °C, each for a duration of 3 h. These calcination temperatures were chosen based on prior literature findings by Lei et al. (2021), which indicated that dehydroxylation of clay minerals—a critical factor in improving pozzolanic activity—typically begins around 400 °C. Moreover, it was noted that temperatures beyond 900 °C lead to a significant reduction in pozzolanic reactivity, likely due to crystallization or sintering of the clay structure, making 800 °C a reasonable upper limit for evaluation. The controlled heating was performed in an electric furnace, and the samples were allowed to cool naturally to room temperature within the furnace to avoid thermal shock.

To evaluate the chemical composition of the materials used in this study, X-ray fluorescence (XRF) analysis was conducted on raw and calcined montmorillonite as well as pyrolyzed coffee grounds (PCG). The analysis provided a detailed determination of the major oxide compositions, with particular attention to SiO_2 (silicon dioxide), Al_2O_3 (aluminum oxide), and Fe_2O_3 (iron oxide), which are key indicators of pozzolanic potential. The results, summarized in Table 2, revealed that the combined content of these oxides in both the raw and thermally treated montmorillonite samples exceeded 70% by weight, thereby satisfying the minimum chemical requirement for natural pozzolanic materials specified by ASTM C618 (Hai and Wang, 2024). This standard establishes the criteria for natural pozzolans used in cement-based systems, ensuring adequate silica and alumina content to promote secondary hydration reactions with calcium hydroxide produced during cement hydration.

In addition to montmorillonite, the pyrolyzed coffee grounds (PCG) were also characterized using XRF to determine their mineral composition after thermal treatment. The results indicate that PCG contains appreciable amounts of silica, calcium, and potassium oxides, reflecting the mineral residues remaining after pyrolysis. Although PCG does not strictly satisfy the ASTM C618 pozzolanic oxide threshold, its porous carbonaceous structure and mineral composition enable it to function primarily as a micro-filler and internal curing agent within the cementitious matrix.

The relatively high oxide content, particularly the elevated levels of SiO_2 and Al_2O_3, suggests that both raw and calcined montmorillonite possess considerable pozzolanic potential. However, calcination further enhances these properties by disrupting the clay's crystalline structure and increasing the availability of reactive aluminosilicate phases. As a result, thermally activated montmorillonite can serve as an effective supplementary cementitious material (SCM) for partial cement replacement in concrete composites.

When combined with PCG, the calcined montmorillonite contributes to a synergistic improvement in the microstructure of the cement matrix. The reactive aluminosilicate phases participate in pozzolanic reactions with calcium hydroxide to form additional calcium silicate hydrate (C–S–H) and calcium aluminosilicate hydrate (C–A–S–H) gels, while the porous PCG particles assist in moisture retention and pore refinement. Consequently, the incorporation of both materials can enhance mechanical performance, durability, and sustainability of the concrete while simultaneously reducing the environmental impact associated with cement production.

2.2 Experimental program

2.2.1 Materials characterization

The montmorillonite used in this study was sourced from clay deposits located in Tanga and Arusha, northern Tanzania, regions characterized by abundant and geologically comparable clay resources suitable for construction and engineering applications. Both locations belong to the same clay-bearing geological belt, and sampling was conducted from a continuous and mineralogically uniform deposit. To minimize potential variability, the collected material was treated as a single source, thoroughly homogenized, and processed under identical conditions prior to use.

Following collection, the raw clay was air-dried under ambient laboratory conditions, mechanically ground using a laboratory ball mill, and sieved through a No. 325 mesh (45 μm) sieve to obtain a uniform particle size distribution. This fineness complies with ASTM C618 requirements for pozzolanic materials and ensured material homogeneity, thereby providing a consistent basis for evaluating the effects of thermal activation.

Thermal activation was performed by calcining the prepared montmorillonite in an electric muffle furnace at 400 °C, 600 °C, and 800 °C for a duration of 3 hours. After calcination, the samples were allowed to cool naturally inside the furnace to prevent thermal shock. These temperature levels were selected based on established literature indicating that dehydroxylation of clay minerals initiates at approximately 400 °C, while the formation of highly reactive amorphous aluminosilicate phases is maximized within the range of 600 °C–800 °C. Calcination beyond 900 °C is known to promote recrystallization and phase transformation into less reactive crystalline forms; therefore, 800 °C was adopted as the upper limit for optimal pozzolanic activation.

The chemical composition of both raw and calcined montmorillonite samples was determined using X-ray fluorescence

10.3389/fmats.2026.1755011

TABLE 2 Chemical composition of cement used and montmorillonite.

Oxide (%)	OPC	Raw montmorillonite	Calcined 400 °C	Calcined 600 °C	Calcined 800 °C	PCG (350 °C)
SiO_2	17.57	50.51	52.17	53.50	57.30	34.85
Al_2O_3	4.07	12.62	13.29	13.31	10.93	6.42
Fe_2O_3	3.63	7.81	7.05	6.95	9.05	3.21
CaO	60.48	1.91	3.89	5.19	7.75	14.63
MgO	0.41	6.38	5.62	5.79	6.00	3.75
SO_3	1.79	0.13	0.06	0.07	0.10	0.18
K_2O	0.11	2.02	2.42	2.58	2.35	9.85
Na_2O	0.04	2.88	3.21	3.29	3.49	1.42
TiO_2	0.29	1.00	0.89	0.93	0.92	0.41
P_2O_5	0.13	0.34	0.23	0.25	0.21	1.86
LOI	10.74	10.74	9.93	4.30	2.18	18.42
Residue at 45 μm	12.49	1.72	0.31	1.26	0.80	2.05

(XRF) analysis. The combined content of SiO_2, Al_2O_3, and Fe_2O_3 exceeded 70% for all samples, satisfying the requirements of ASTM C618 for natural pozzolans. Calcination resulted in a reduction in loss on ignition (LOI), attributed to the removal of structural and adsorbed water, along with a slight increase in CaO content, indicating enhanced pozzolanic potential.

Physical properties were evaluated through measurements of specific surface area and specific gravity. Brunauer–Emmett–Teller (BET) analysis showed that the specific surface area increased from 32.5 m^2/g in the raw clay to 61.7 m^2/g after calcination at 800 °C, confirming increased fineness and a higher density of available reactive sites. Specific gravity, determined using the Le Chatelier method, increased from 2.53 g/cm^3 for the raw montmorillonite to 2.70 g/cm^3 after calcination at 800 °C, suggesting structural densification and improved particle packing.

Microstructural and mineralogical transformations induced by calcination were investigated using Fourier-transform infrared spectroscopy (FTIR), X-ray diffraction (XRD), and scanning electron microscopy (SEM). FTIR spectra recorded in the range of 400–4,600 cm^{-1} showed a progressive reduction in OH-stretching bands with increasing temperature, along with a shift in the Si–O stretching vibration from approximately 984 cm^{-1} in the raw montmorillonite to about 1,040 cm^{-1} at 800 °C, indicating increased structural disorder and amorphization. XRD patterns revealed a gradual loss of characteristic crystalline montmorillonite peaks and the development of broad diffuse humps, particularly at 800 °C, which are indicative of amorphous aluminosilicate phases. SEM micrographs supported these observations, showing a transformation from well-defined plate-like layered structures in the raw clay to fragmented, denser, and more uniformly dispersed amorphous particles at higher calcination temperatures.

Overall, these results demonstrate that calcination significantly enhances the reactivity of montmorillonite by increasing surface area, reducing crystallinity, and promoting the formation of amorphous aluminosilicate phases capable of reacting with calcium hydroxide during cement hydration. This transformation confirms the suitability of calcined montmorillonite as a sustainable supplementary cementitious material, with strong potential to improve both the mechanical performance and durability of concrete.

2.3 Experimental program

The experimental program was designed to systematically evaluate the influence of montmorillonite calcination temperature and cement replacement level on the mechanical, durability, and microstructural performance of concrete incorporating coffee biochar. To ensure that the observed variations in performance were directly attributable to these intended variables, other key mixture parameters were deliberately fixed and are scientifically justified below. This controlled approach minimizes confounding factors and strengthens the reliability of the comparative analysis.

Concrete mixtures were prepared using Ordinary Portland Cement (CEM I 32.5 R), natural river sand, potable mixing water, montmorillonite (raw and calcined), and pyrolyzed coffee grounds (PCG). The coffee waste was thermally treated at 350 °C under oxygen-limited conditions, producing coffee biochar rather than combustion ash. This distinction is important because pyrolysis produces a partially carbonized, porous carbonaceous material with different physicochemical characteristics compared with mineral ash obtained from complete combustion. Accordingly, the material is referred to throughout this study as coffee biochar (PCG biochar).

The coffee biochar was used as a constant 15% replacement of fine aggregate in all mixtures. This replacement level was selected based on both prior literature and mechanistic considerations. Several studies have reported that approximately 15% biochar replacement provides a favorable balance between mechanical strength retention, durability improvement, and microstructural refinement. At a pyrolysis temperature of around 350 °C, most volatile compounds are removed while a stable, partially carbonized porous structure is retained. This structure enables biochar particles to act primarily as micro-fillers and localized moisture reservoirs, contributing to internal curing and pore refinement within the cementitious matrix.

Replacement levels lower than this threshold typically produce limited filler and densification effects, resulting in marginal improvements in performance. In contrast, higher replacement levels can disrupt the load-bearing aggregate skeleton, increase porosity, and reduce compressive strength due to the comparatively lower stiffness and density of biomass-derived particles relative to natural sand. Fixing the coffee biochar content at 15% therefore ensures mechanical stability, enhances reproducibility, and avoids confounding effects associated with variations in aggregate volume fraction.

The water-to-cement ratio was also maintained constant throughout the study to eliminate variability in hydration kinetics and pore structure development. Since the w/c ratio strongly governs strength, permeability, and durability, keeping it fixed ensures that changes in performance are directly associated with montmorillonite calcination temperature and replacement level rather than variations in matrix water content.

By maintaining consistent PCG biochar content, aggregate grading, curing conditions, and mixing procedures, the experimental design isolates the effect of montmorillonite thermal activation. This structured methodology enhances the validity of the statistical analysis and supports robust interpretation of the influence of calcination temperature on pozzolanic reactivity, matrix densification, and long-term durability performance (Rashid et al., 2024; Rashidi et al., 2024; Shamsa et al., 2022).

The water-to-cement (w/c) ratio was fixed at 0.485 for all mixtures to ensure consistent hydration conditions, comparable workability, and controlled pore structure development across the experimental matrix. In cementitious systems incorporating montmorillonite and coffee biochar, water demand is strongly influenced by the high specific surface area, layered structure, and adsorption capacity of clay minerals, as well as the internal porosity of biochar particles. These materials absorb part of the mixing water, reducing the effective free water available for cement hydration and compaction.

In conventional mortar and concrete systems, the practical allowable w/c range for structural applications typically varies between approximately 0.40 and 0.55, depending on strength and durability requirements. Ratios below about 0.40 may lead to inadequate workability and incomplete hydration without the use of superplasticizers, while ratios above approximately 0.55 significantly increase capillary porosity and permeability, thereby reducing strength and long-term durability.

Considering the additional water absorption associated with montmorillonite and coffee biochar, a w/c ratio of 0.485 was selected as a controlled mid-range value within the allowable practical range. This value compensates for adsorption effects while avoiding excessive free water that could artificially increase porosity and obscure the influence of calcination temperature.

If a lower w/c ratio had been adopted, insufficient effective water could have resulted in reduced workability and microstructural defects. Conversely, a higher ratio would increase capillary pore connectivity and susceptibility to durability deterioration. By maintaining a constant w/c ratio of 0.485 across all mixtures, variations in strength and durability can be confidently attributed to calcination-induced phase transformation, pozzolanic reactivity, and matrix densification, rather than uncontrolled differences in water content (Wang and Zhang, 2025; Wang et al., 2019).

The sand content was also kept constant across all mixtures to eliminate the influence of aggregate packing density and interfacial transition zone variability, both of which strongly affect strength and permeability. Fixing the fine aggregate content allowed the experimental program to isolate the effects of binder modification and ensured meaningful comparison between mixtures.

Montmorillonite was incorporated in raw form and after calcination at 400 °C, 600 °C, and 800 °C, replacing cement at 5%, 10%, 15%, and 20% by mass. A control mixture without montmorillonite was also prepared. All mixtures were produced following ASTM-recommended mixing, casting, and curing procedures to ensure reproducibility.

The experimental program included mechanical testing (compressive, tensile, and flexural strength, and Vickers hardness), durability evaluation (acid attack, chloride exposure, corrosion potential, and residual strength after thermal exposure), and microstructural characterization using FTIR, XRD, and SEM. To quantitatively assess the individual and interactive effects of calcination temperature and replacement level, all experimental results were analyzed using two-way analysis of variance (ANOVA).

2.3.1 Compressive strength (fc)

Compressive strength measures the ability of a material to withstand loads that tend to reduce size. It was determined using Equation 1:

$$\mathrm{Fc} = \frac{P}{A} \tag{1}$$

Where:

Fc = compressive strength (in N/mm2 or MPa).

P = maximum load applied to the specimen (in Newtons).

A = cross-sectional area of the cube (in mm^2). For a 50 mm × 50 mm cube, A = 2,500 mm^2

2.3.2 Tensile strength (Tt)

Tensile strength assesses a material's resistance to axial tension and was determined using prism samples. The formula used is given in Equation 2:

$$\mathrm{Fc} = \frac{2P}{\pi \mathrm{DL}} \tag{2}$$

Where:

Ft = tensile strength (in N/mm2 or MPa).

P = maximum load applied to the specimen (in Newtons). d = width of the specimen (in mm).

L = length of the specimen (in mm).

This equation applies when cylindrical or split tensile specimens are not used and prisms are employed for direct tensile testing.

2.3.3 Flexural strength (modulus of rupture) (Fr)

Flexural strength reflects a material's resistance to bending and is calculated using Equation 3:

$$\mathrm{Fr} = \frac{3PL}{2\mathrm{bd}^2} \tag{3}$$

Where:

Fr = flexural strength (in N/mm2 or MPa).

P = maximum load applied at the center of the prism (in Newtons). L = span length between supports (typically 100 mm).

b = width of the prism (40 mm).

d = depth (height) of the prism (40 mm).

2.3.4 Strength loss at elevated temperatures

This metric evaluates the reduction in compressive strength due to thermal exposure as shown in Equation 4:

$$Strength\ Loss\ (\%) = \frac{F_C\ (ref) - F_C\ (T)}{F_C\ (ref))} \quad (4)$$

Where:

$F_{c\ (ref)}$ = compressive strength at room temperature (reference value). Fc (T) = compressive strength after exposure to elevated temperature. The result is expressed as a percentage loss in strength.

2.3.5 Mass loss percentage

This is used to assess durability by measuring how much mass a specimen loses after immersion in acidic or saline environments as given in Equation 5:

$$Mass\ Loss\ (\%) = \frac{M_{ii} - M_f}{M_j)} \times 100 \quad (5)$$

Where: (M_i - M_f).

M_i = initial mass before exposure (in grams). M_f = final mass after exposure (in grams).

The result indicates material degradation as a percentage of mass lost.

2.3.6 Residual strength percentage

This measures how much strength remains after exposure to aggressive conditions (e.g., acid, salt) as expressed in Equation 6:

$$Residual\ Strength\ (\%) = \frac{F_C(\exp)}{F_C(ref)} \times 100 \quad (6)$$

Where:

Fc (exp) = compressive strength after exposure to aggressive environment. Fc (ref) = reference compressive strength under standard conditions.

The result shows the percentage of strength retained. The mix proportions and quantities of materials used for sample preparation are presented in Table 3.

2.3.7 Physical behavior of calcined montmorillonite and pyrolyzed coffee grounds (PCG)

The specific surface area and specific gravity of montmorillonite are key physical behavior that significantly influence its performance in cement composites. Specific surface area refers to the total surface area available per unit mass of the material. A higher specific surface area means the material has more reactive sites available for chemical interaction during cement hydration. In this study, the specific surface area was determined using a Brunauer–Emmett–Teller (BET) surface area analyzer in accordance with ISO 9277:2010, which measures nitrogen adsorption to evaluate the available surface area with high precision.

When montmorillonite is thermally activated through calcination, its crystalline layered structure breaks down, causing an increase in surface area and resulting in finer, more amorphous particles. This enhanced surface area promotes greater pozzolanic reactivity by facilitating the formation of additional cementitious compounds such as calcium silicate hydrate gels, which contribute to a denser and stronger microstructure. However, an increase in surface area also tends to increase the water demand of the mix, which can affect fresh properties such as workability.

Specific gravity, on the other hand, represents the density of the material relative to water and provides insight into the material's solid phase volume and packing within the concrete matrix. In this work, the specific gravity was measured using a Le Chatelier flask apparatus in accordance with ASTM C188 or EN 196–6, which determine the volume displaced by a known mass of the material in kerosene or water. After calcination, montmorillonite typically exhibits a slight increase in specific gravity due to the densification and loss of hydroxyl groups in its structure. This higher density helps improve particle packing and reduces the overall porosity of the cement matrix, resulting in improved mechanical strength and durability. Furthermore, knowing specific gravity allows for precise calculation of volumetric replacement in mix designs, ensuring consistent and optimized concrete properties.

Together, these two physical properties—specific surface area and specific gravity—play a crucial role in determining how montmorillonite interacts within cementitious systems. The increased surface area enhances chemical reactivity and secondary hydration product formation, while the specific gravity affects volume stability and matrix compactness. Their combined effect leads to improved strength, lower permeability, and better durability of concrete containing calcined montmorillonite. Understanding and controlling these properties are essential for optimizing the use of montmorillonite as a sustainable supplementary cementitious material.

2.3.8 Specific surface area

Specific surface area (SSA) represents the total surface area available per unit mass of a material and serves as a critical indicator of its reactivity. For pozzolanic materials such as montmorillonite, a higher SSA provides more active sites for interaction with calcium hydroxide released during cement hydration, thereby enhancing the formation of additional cementitious products like calcium silicate hydrate (C–S–H) and calcium aluminate silicate hydrate (C–A–S–H) gels.

In its natural form, montmorillonite exhibits a relatively low surface area due to its compact, layered crystalline structure. Upon calcination, however, the dehydration and partial collapse of this layered framework promote structural breakdown, producing finer and more amorphous particles with a significantly larger reactive surface. The increase in surface area following thermal activation facilitates faster and more extensive pozzolanic reactions, resulting in a denser, more cohesive microstructure with improved mechanical performance and durability as explained in Table 4.

10.3389/fmats.2026.1755011

TABLE 3 Material used for sample preparation.

Sample	W/C	Cement (g)	Sand (g)	Raw M (g)	M400 (g)	M600 (g)	M800 (g)
Control	0.485	2,400	6,600	0	0	0	0
S5Mraw	0.485	2,280	6,600	120	0	0	0
S10Mraw	0.485	2,160	6,600	240	0	0	0
S15Mraw	0.485	2040	6,600	360	0	0	0
S20Mraw	0.485	1920	6,600	480	0	0	0
S5M400	0.485	2,280	6,600	0	120	0	0
S10M400	0.485	2,160	6,600	0	240	0	0
S15M400	0.485	2040	6,600	0	360	0	0
S20M400	0.485	1920	6,600	0	480	0	0
S5M600	0.485	2,280	6,600	0	0	120	0
S10M600	0.485	2,160	6,600	0	0	240	0
S15M600	0.485	2040	6,600	0	0	360	0
S20M600	0.485	1920	6,600	0	0	480	0
S5M800	0.485	2,280	6,600	0	0	0	120
S10M800	0.485	2,160	6,600	0	0	0	240
S15M800	0.485	2040	6,600	0	0	0	360
S20M800	0.485	1920	6,600	0	0	0	480

TABLE 4 Specific surface area.

Sample	Thermal treatment temperature (°C)	Specific surface area (m^2/g)
Raw montmorillonite (uncalcined)	Raw	32.5
Montmorillonite calcined	400	45.8
Montmorillonite calcined	600	54.3
Montmorillonite calcined	800	61.7
Pyrolyzed coffee grounds (PCG)	350	16.8

Nevertheless, a higher surface area can also increase the water demand of the mix, as the extensive particle surfaces require additional water to achieve suitable workability. Therefore, mix proportion adjustments may be necessary to maintain consistency and flow properties.

The measured BET surface area values in this study (Table 4) confirmed a progressive increase with calcination temperature—from 32.5 m^2/g for raw montmorillonite to 61.7 m^2/g at 800 °C. The pyrolyzed coffee grounds (PCG) at 350 °C exhibited a specific surface area of 16.8 m^2/g, indicating moderate fineness that complements the reactive potential of the calcined clay. This enhancement in surface characteristics underscores the critical role of calcination in improving the physicochemical performance of montmorillonite as a sustainable supplementary cementitious material.

2.3.9 Specific gravity

Specific gravity (SG) is defined as the ratio of the density of a material to the density of water at a specified temperature. It reflects the intrinsic density of the solid particles and plays an essential role in determining the volumetric proportioning and packing characteristics of cementitious materials. In mix design, accurate knowledge of specific gravity ensures proper volumetric replacement when supplementary cementitious materials (SCMs) such as montmorillonite are used to partially substitute cement.

For montmorillonite, specific gravity provides insight into its microstructural compactness and the degree of densification achieved during calcination. Thermal activation leads to structural transformations such as dehydroxylation and removal of volatile constituents, which result in a denser and more stable amorphous phase. Consequently, the specific gravity of montmorillonite increases with calcination temperature, reflecting improved particle consolidation and reduced internal voids.

In this study, the specific gravity of raw montmorillonite was measured at 2.53 g/cm^3, while calcination at 400 °C, 600 °C, and 800 °C increased it progressively to 2.60, 2.65, and 2.70 g/cm^3, respectively (Table 5). This rise in density indicates enhanced structural packing and a stronger solid framework. In contrast, the pyrolyzed coffee grounds (PCG) exhibited a lower specific gravity of 1.85 g/cm^3 at 350 °C, consistent with their porous carbonaceous structure.

The increase in montmorillonite density after calcination contributes to improved packing efficiency and reduced porosity within the cement matrix. A denser microstructure minimizes pore connectivity and enhances the mechanical strength and durability of the composite. Conversely, neglecting differences in specific gravity during mix design could result in inaccurate

10.3389/fmats.2026.1755011

TABLE 5 Specific gravity.

Sample	Thermal treatment temperature (°C)	Specific gravity (g/cm^3)
Raw montmorillonite (uncalcined)	Raw (0)	2.53
Montmorillonite calcined	400	2.60
Montmorillonite calcined	600	2.65
Montmorillonite calcined	800	2.70
Pyrolyzed coffee grounds (PCG)	350	1.85

volumetric proportions, leading to undesirable variations in workability, strength, and long-term performance as explained in Table 5.

Overall, the observed increase in specific gravity with calcination temperature confirms the structural densification and enhanced pozzolanic potential of montmorillonite, reinforcing its suitability as a high-performance, thermally activated SCM for sustainable concrete applications.

3 Methods

The methodology of this study involved a systematic approach to evaluate the performance of raw and calcined montmorillonite in concrete formulations under various hazardous environments.

3.1 Reactivity of raw and calcined montmorillonite

For raw and calcined montmorillonite, Fourier transform infrared spectroscopy (FTIR) and X-ray diffraction (XRD) characterization were conducted to evaluate reactivity changes due to calcination. The Analytical X′Pert Pro X-Ray diffractometer was used with a setup of 30 mA and 40 kV, analyzing mineralogical phases by diffraction peaks over a large 2θ range of 10°–90°. An A224159 SHIMADZU Fourier transform infrared spectrophotometer recorded the percentage of transmittance peaks versus wavelengths between 400 and 4,600 cm^{-1}.

Powder samples of raw and different calcilead montmorillonite, passing through a number 325 sieve, were utilized for both methods. montmorillonite.

3.2 Fresh bulk density

The results show that incorporating both calcined and raw montmorillonite in concrete reduces the fresh bulk density compared to the control mixture. A significant reduction in fresh bulk density is observed as the montmorillonite content increases from 5% to 20%. This is primarily due to the lower specific gravity of montmorillonite compared to cement, which leads to a reduction in the overall mass per unit volume of the concrete mixture.

This reduction in fresh bulk density can be attributed to several factors. Montmorillonite has a layered silicate structure and high surface area, which increases the water demand of the mix, thereby affecting its workability and compaction. Additionally, the finer particle size of montmorillonite compared to cement contributes to a higher volume of paste with lower mass, leading to a lower density. The pozzolanic reactivity of calcined montmorillonite allows it to partially replace cement while contributing to the formation of additional calcium silicate hydrate (C–S–H) gel, although this primarily influences long-term strength rather than fresh density (Langaroudi and Mohammadi, 2018).

The reduction in fresh bulk density may also result from decreased water content at higher montmorillonite replacement levels, as montmorillonite absorbs more water due to its high specific surface area. This alters the mix water-to-binder ratio and can slightly reduce compaction efficiency. Moreover, increasing the calcination temperature of montmorillonite further reduces the fresh bulk density of the concrete. This is due to the breakdown of montmorillonite structure at higher temperatures, resulting in finer, more porous particles that replace the denser cement particles and occupy more volume with less mass.

3.3 Reactivity of raw and calcined montmorillonite

For raw and calcined montmorillonite, Fourier transform infrared spectroscopy (FTIR) and X-ray diffraction (XRD) characterization were conducted to evaluate reactivity changes due to calcination. The Analytical X′Pert Pro X-Ray diffractometer was used with a setup of 30 mA and 40 kV, analyzing mineralogical phases by diffraction peaks over a large 2θ range of 10°–90°. An A224159 SHIMADZU Fourier transform infrared spectrophotometer recorded the percentage of transmittance peaks versus wavelengths between 400 and 4,600 cm^{-1}.

Powder samples of raw and different calcined bentonite, passing through a number 325 sieve, were utilized for both methods. montmorillonite.

3.4 Fresh property

The fresh bulk density of pozzolana incorporation is linked to the reactivity of pozzolana with calcium hydroxide to form hydrated calcium silicate. Higher surface area leads to greater pozzolanic reactivity, resulting in lower fresh bulk density of cementing materials. The fresh density for both raw and calcined montmorillonites blended mortar was measured using a one-litre cylinder to determine the volume of the mortar sample.

3.5 Hardened properties

The hardened properties of the montmorillonite-blended concrete were evaluated through compressive strength, tensile strength, flexural strength, strength activity index (SAI), Vickers hardness, chemical resistance, and thermal resistance tests. These tests were designed to assess both mechanical performance and durability under aggressive environmental conditions.

Cube specimens measuring 50 × 50 × 50 mm^3 were prepared for compressive strength testing, while prism specimens of 40 × 40 × 160 mm^3 were used for flexural strength evaluation. All specimens were demolded 24 h after casting and subsequently cured in water at a controlled temperature of 25 °C ± 2 °C until the designated testing age. For each mix proportion and each curing age, three replicate specimens were tested, and the average value was reported. Standard deviations were calculated to assess variability and ensure statistical reliability of the results.

Compressive strength testing was conducted in accordance with ASTM C109, using a Zwick-Roell digital compressive strength machine at a loading rate of 1800 N/s. Flexural strength tests were performed using a DKZ-5000 electronic flexural testing machine following ASTM C348 procedures. The mechanical properties were evaluated at curing ages of 28, 56, and 90 days to assess both medium- and long-term performance.

The Strength Activity Index (SAI) at 28 days was determined to quantify the pozzolanic contribution of raw and calcined montmorillonite. It was was calculated using Equation 7:

$$\text{SAI}\,(\%) = \frac{\text{fc, MMT}}{\text{fc, Control}} \times 100 \tag{7}$$

where $f_{c,\,MMT}$ is the compressive strength of the mortar containing montmorillonite and $f_{c,Control}$ is the compressive strength of the control mortar at 28 days.

Vickers hardness testing was performed using a diamond-shaped indenter under controlled loading conditions. The hardness value (HV) was calculated using Equation 8:

$$\text{HV} = \frac{1.854\,\text{F}}{\text{d}^2} \tag{8}$$

where F is the applied load (kgf) and d is the mean diagonal length of the indentation (mm).

For durability assessment, mortar cubes (150 × 150 × 150 mm^3) were immersed in 5% HCl, 5% HNO_3, and 10% NaCl solutions for 90 days. Mass loss and residual compressive strength were determined after exposure. Thermal resistance was evaluated by exposing cured specimens to 200 °C for 2 h, followed by measurement of residual compressive strength.

All experimental results were statistically analyzed using two-way ANOVA to evaluate the independent and interaction effects of calcination temperature and replacement level.

Additionally, the Vickers hardness test was conducted by indenting the test materials with a diamond-shaped indenter, and Vickers hardness was evaluated using Equation 9:

$$\text{HV} = \frac{\mathbf{2F}\sin(\boldsymbol{\theta}/\mathbf{2})}{2\text{d}^2} = \frac{1.854\,\text{F}}{\text{d}^2} \tag{9}$$

In this study, the load (F) is measured in kgf, the arithmetic mean of the two diagonals of the indented area (d) is measured in mm, and Vickers hardness (HV) is expressed in kgf/mm^2.

The acid attack test involved concrete specimens sized at 150 mm^3, which were immersed for 90 days in a 5% acid solution made from hydrochloric acid and nitric acid. The weights of all cubes were recorded before immersion, and they remained in the acidic solutions for a total of 90 days. After this period, the mortar specimens were removed from the acids and allowed to dry at room temperature for 24 h. Following drying, the compressive strength tests were conducted, and the resistance to acid attack was determined by comparing the mass loss of the cubes and the strength loss against samples that had been cured in water as illustrated in Table 6.

For the salt attack test, two plain mortar cubes and one mortar cube containing an embedded steel bar were prepared using raw and calcined montmorillonite blended mortar and then immersed in a 10% NaCl solution. After 90 days of immersion, the samples were taken out and left to dry at room temperature for 24 h. The mass loss resulting from the salty environment was recorded, and the corrosion resistance of the steel bars was assessed through visual inspection of their surfaces, considering different doses of raw and calcined montmorillonite.

Additionally, the impact of elevated temperature was studied using a 50 mm^3 mortar specimen, which was placed in an electronic oven at 200 °C for 2 hours after curing for 90 days. The mass change before and after exposure to the elevated temperature was documented, followed by a compressive strength test.

3.6 Result and discussions

3.6.1 Microstructural and physicochemical characterization

Comprehensive chemical and microstructural characterization was performed to understand the mechanisms governing the superior performance of montmorillonite-blended concretes. The combined use of Fourier Transform Infrared Spectroscopy (FTIR), X-ray Diffraction (XRD), and Scanning Electron Microscopy (SEM) provided complementary evidence of the physicochemical evolution of the binder system as a function of calcination temperature (T), replacement level (R), and their interaction (T × R). The analyses confirmed that calcination between 600 °C and 800 °C produced highly reactive amorphous aluminosilicates that promoted extensive pozzolanic activity, resulting in refined microstructures, reduced porosity, and increased phase stability.

3.6.2 FTIR analysis

Fourier transform infrared (FTIR) spectroscopy was used to assess the chemical structural changes induced by calcination of montmorillonite and their interaction with coffee ash in the blended concrete system. As shown in Figure 1, raw montmorillonite exhibits a broad band at approximately 3,383 cm^{-1} corresponding to O–H stretching vibrations of structural hydroxyl groups and interlayer water, while the band near 1,634 cm^{-1} is associated with H–O–H bending vibrations of adsorbed water, reflecting a hydrated and structurally ordered clay matrix.

After calcination at 400 °C, the intensity of hydroxyl-related bands decreased, indicating partial dehydroxylation and removal of physically bound water. This change marks the initial thermal activation of the clay structure and the decomposition of volatile species, including residual organic and carbonate-related components associated with coffee ash, as reflected by the reduced intensity of the band around 2,361 cm^{-1} (Langaroudi and Mohammadi, 2018).

At higher calcination temperatures (600 °C–800 °C), hydroxyl bands were significantly weakened or absent, confirming extensive

TABLE 6 Testing conditions for concrete mixtures.

Test category	Test type	Specimen size (mm)	Specimens per age/Condition	Total specimens per mix	Curing/Exposure condition	Testing age/Duration	Standard followed
Fresh properties	Slump test	Standard slump cone (100/200/300 height)	3 trials	3	Tested immediately after mixing	Fresh state	ASTM C143
	Fresh density	7-L density mold	3 trials	3	Tested immediately after mixing	Fresh state	ASTM C138
Mechanical properties	Compressive strength (cube)	150 × 150 × 150 cubes	3 per age	9 (28, 56, 90 days)	Water curing at 27 °C ± 2 °C after 24 h demolding	28, 56, 90 days	EN 12390–3
	Compressive strength (cylinder)	150 × 300 cylinders	3 per age	9	Water curing at 27 °C ± 2 °C	28, 56, 90 days	ASTM C39
	Split tensile strength	150 × 300 cylinders	3 per age	9	Water curing at 27 °C ± 2 °C	28, 56, 90 days	ASTM C496
	Flexural strength	100 × 100 × 500 beams	3 per age	9	Water curing at 27 °C ± 2 °C	28, 56, 90 days	ASTM C78
	Vickers hardness	Polished concrete surface	3 specimens	3	Tested after curing	28 and 90 days	ASTM E384
Durability properties	Acid resistance (5% HCl & HNO_3)	150 × 150 × 150 cubes	3 specimens	3	Immersion in acid solution	90 days immersion	—
	Chloride/Salt resistance	150 × 150 × 150 cubes (with embedded steel bar)	3 specimens	3	Immersion in 10% NaCl solution	90 days immersion	ASTM C876
	Thermal exposure	150 × 150 × 150 cubes	3 specimens	3	Oven heating at 200 °C for 2 h after 90 days curing	Post-exposure testing	—
Microstructural analysis	FTIR	Powder samples (<75 μm)	—	—	Oven-dried before analysis	After calcination	Instrumental analysis
	XRD	Powder samples (<75 μm)	—	—	Dried samples	After calcination	XRD analysis
	SEM	Fractured concrete surface	—	—	Gold-coated before imaging	After curing	SEM imaging

10.3389/fmats.2026.1755011

dehydroxylation and collapse of the original aluminosilicate framework. Simultaneously, the dominant Si–O stretching vibration intensified and shifted toward ~1,032 cm^{-1}, accompanied by band broadening. This behavior indicates the formation of disordered, amorphous Si–O–Al linkages derived from both calcined montmorillonite and the silica-rich fraction of coffee ash. The attenuation of the 916 cm^{-1} band, associated with Al–Al–OH bending, further confirms breakdown of octahedral layers.

These molecular-scale transformations directly explain the enhanced mechanical performance of the coffee ash concrete composites. The generation of amorphous aluminosilicate phases increases the availability of reactive silica and alumina, which readily participate in pozzolanic reactions with calcium hydroxide released during cement hydration. The resulting formation of secondary C–S–H and C–A–S–H gels leads to pore refinement and matrix densification, strengthening the interfacial transition zone and improving compressive, tensile, and flexural strength (Abdalla et al., 2023).

From a durability perspective, the extensive dehydroxylation and amorphization observed at elevated calcination temperatures promote accelerated calcium hydroxide consumption and reduce the content of portlandite vulnerable to acid and chloride attack. The combined effect of reduced pore connectivity and stable secondary hydration products limits the ingress of aggressive ions, thereby enhancing long-term durability. The FTIR trends observed in this study are consistent with those reported for blended systems incorporating fly ash and metakaolin, where amorphization and calcium hydroxide consumption similarly govern strength and durability enhancement.

The progression from raw to 800 °C calcined montmorillonite clearly shows how thermal treatment impacts the material's chemistry and structure. The raw montmorillonite, with high water and hydroxyl content, is the least thermally stable. 1ncreasing the calcination temperature progressively removes water and hydroxyl groups, converts the clay to a more stable phase, and improves material properties such as thermal stability, purity, and suitability for advanced applications. The 800 °C calcined sample is the best in terms of complete dehydroxylation and structural stability, followed by the 600 °C sample, which offers a good structural balance, then 400 °C with partial changes, and finally the raw sample, which remains largely hydrous and structurally unaltered. This data is critical for tailoring montmorillonite for specific industrial applications where thermal stability and surface characteristics are key parameters (Ahmed, 2024).

Overall, FTIR analysis confirms that calcination transforms montmorillonite into a chemically reactive aluminosilicate phase that interacts synergistically with coffee biochar, providing a molecular-level basis for the improved mechanical and durability performance of the concrete composites.

3.6.3 XRD analysis

X-ray diffraction (XRD) analysis was carried out to investigate the phase evolution of montmorillonite induced by calcination and to establish its role in controlling the mechanical and durability performance of the concrete composites. The diffraction pattern of raw montmorillonite exhibited sharp and well-defined peaks characteristic of a crystalline layered aluminosilicate structure. Such

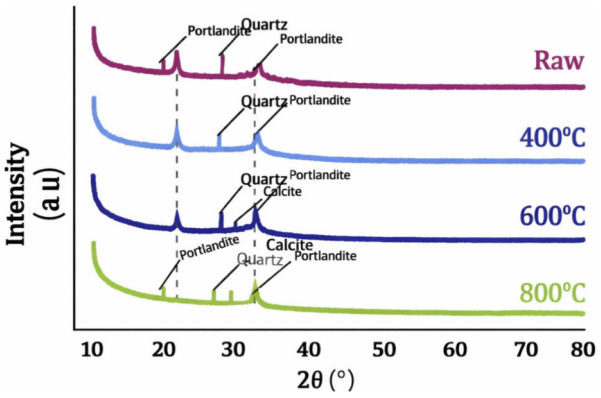

FIGURE 2
XRD analysis.

a highly ordered structure is chemically stable and therefore exhibits limited pozzolanic reactivity, as the silica and alumina are strongly bound within the crystal lattice.

After calcination at 400 °C, a noticeable reduction in peak intensity was observed, indicating the onset of dehydroxylation and partial disruption of the layered structure. At this temperature, removal of structural hydroxyl groups weakens interlayer bonding and initiates lattice collapse; however, the persistence of crystalline peaks suggests that the transformation remains incomplete, limiting the extent of reactivity enhancement (Abdalla et al., 2023).

At 600 °C, the diffraction peaks became significantly broadened and less intense, reflecting a pronounced loss of crystallinity and the formation of disordered aluminosilicate phases. This structural amorphization is critical for strength development, as it increases the availability of reactive silica and alumina capable of participating in pozzolanic reactions with calcium hydroxide released during cement hydration. The formation of secondary C–S–H and C–A–S–H gels resulting from these reactions leads to mechanistic explanation ($Ca(OH)_2$ consumption + pore refinement), densification of the cement matrix, and strengthening of the interfacial transition zone, thereby directly explaining the observed increase in mechanical strength (Langaroudi and Mohammadi, 2018).

At 800 °C, most characteristic montmorillonite peaks disappeared and were replaced by broad diffuse humps, indicating the predominance of amorphous aluminosilicate phases. This phase transformation plays a decisive role in durability performance. The highly amorphous structure promotes extensive consumption of calcium hydroxide, reducing the amount of portlandite that is vulnerable to acid and chloride attack. In addition, the formation of stable secondary hydration products reduces pore connectivity and permeability, limiting the ingress of aggressive ions. Therefore, the development of amorphous aluminosilicate phases is identified as the key phase change governing durability enhancement as explained in Figure 2.

The raw montmorillonite is the least effective, as it contains mainly crystalline phases with minimal disorder. The presence of quartz, while thermally stable, is essentially inert in cementitious environments, and the crystalline clay lattice does not promote

significant chemical reactivity. Without thermal activation, the material lacks the structural and chemical characteristics necessary to contribute effectively as a supplementary cementitious material (Ndahirwa et al., 2022; Sakir et al., 2020).

In conclusion, the order of effectiveness is clearly 800 °C > 600 °C > 400 °C > Raw. This ranking is justified by the extent of amorphization, dehydroxylation, and phase decomposition revealed by the XRD patterns. The higher the degree of amorphization, the greater the concentration of reactive Si–Al species, which are essential for pozzolanic reactions. Therefore, calcination at 800 °C offers the best pathway for producing highly reactive montmorillonite suitable for cementitious applications, while lower calcination temperatures result in progressively less reactive materials.

3.6.4 SEM Morphological Analysis

Scanning electron microscopy (SEM) was employed to examine the microstructural features of concrete incorporating raw and calcined montmorillonite and to relate these features to mechanical strength and durability performance. The control mixture and concrete containing raw montmorillonite exhibited a relatively loose and heterogeneous microstructure, characterized by visible capillary pores, poorly packed hydration products, and a distinct interfacial transition zone (ITZ). Plate-like clay particles and unreacted phases were still present, indicating limited pozzolanic activity and incomplete microstructural development.

Concrete incorporating montmorillonite calcined at 400 °C showed partial improvement in matrix compactness, with increased formation of hydration products and reduced pore size compared with the raw clay mixture. However, the microstructure remained non-uniform, reflecting incomplete activation of the clay mineral and limited secondary gel formation (Abdalla et al., 2023).

At a calcination temperature of 600 °C, SEM images revealed a markedly denser and more homogeneous microstructure. The cement matrix was dominated by well-distributed C–S–H and C–A–S–H gels, accompanied by significant reduction in capillary porosity and a less pronounced ITZ. This densification is attributed to enhanced pozzolanic reactivity of calcined montmorillonite, which promotes mechanistic explanation ($Ca(OH)_2$ consumption + pore refinement), resulting in improved bonding between the cement paste and aggregates. These microstructural features are comparable to those commonly reported for concrete incorporating established supplementary cementitious materials such as fly ash and metakaolin, where secondary gel formation and pore refinement are the primary mechanisms governing strength enhancement (Langaroudi and Mohammadi, 2018).

Concrete incorporating montmorillonite calcined at 800 °C exhibited the most compact and continuous microstructure, characterized by a dense gel network with minimal microcracks and significantly reduced pore connectivity. The extensive formation of secondary hydration products effectively filled voids and strengthened the ITZ. This refined microstructure is particularly critical for durability performance, as reduced pore connectivity limits the ingress of aggressive agents such as acids and chlorides, while the diminished presence of portlandite-rich regions enhances resistance to chemical attack. Similar durability-related microstructural benefits have been reported for fly ash–and metakaolin-based systems, further supporting the effectiveness of calcined montmorillonite as a comparable supplementary cementitious material (Lei et al., 2021; Rashidi et al., 2024; Ahmed, 2024; DuchesneJ, 2021; Fode et al., 2023). The surface texture becomes rougher and more heterogeneous, facilitating mechanical interlocking and improving load transfer within the composite.

The most pronounced changes are seen in samples calcined at 800 °C. SEM images (Figure 3) illustrate extensive disintegration of montmorillonite platelets into fine, amorphous particles that uniformly distribute throughout the matrix. This treatment effectively creates metakaolin-like phases with high pozzolanic reactivity, as also supported by FTIR and XRD analyses. The microstructure exhibits significant densification with a substantial reduction in microvoids and portlandite crystals, resulting in enhanced bonding at the ITZ and a compact matrix architecture (DuchesneJ, 2021; Fode et al., 2023; Ndahirwa et al., 2022; Sakir et al., 2020).

These microstructural improvements correlate closely with the highest mechanical strengths and durability observed in the (Abdalla et al., 2023).

Overall, SEM analyses provide direct visual evidence that thermal activation of montmorillonite transforms the clay into a highly reactive SCM, contributing to pore refinement, matrix densification, and improved mechanical interlocking within cement composites exposed to diverse environments. However, it is acknowledged that further quantification using mercury intrusion porosimetry (MIP) or Nano indentation could provide deeper insights into pore size distribution and mechanical properties at the microscale, which are recommended for future studies.

3.6.5 Integrated interpretation

The integrated FTIR–XRD–SEM evidence provides a coherent picture of the chemical and structural transformations driving performance enhancement. Dehydroxylation (300 °C–600 °C) leads to breakdown of structural–OH groups; amorphization (600 °C–800 °C) creates a reactive disordered Si–O–Al lattice; hydration reactions produce cross-linked C–A–S–H gels; and microstructural stabilization strengthens ITZs and blocks pores. This sequence—dehydroxylation → amorphization → pozzolanic gel formation → microstructural sealing—explains improvements across all performance categories. The correlation among F-values (temperature > replacement > interaction) from ANOVA, spectral amorphization indices, and microstructural compactness establishes a unified chemical–mechanical mechanism.

3.6.6 Summary and implications

The combined chemical analyses confirm that calcination temperature is the principal driver of reactivity and durability. At 600 °C–800 °C, montmorillonite transitions into an amorphous, reactive aluminosilicate network capable of binding $Ca(OH)_2$ and generating dense, thermally stable gels. These reactions strengthen the C–A–S–H backbone, eliminate portlandite vulnerability, and create fine interlocked microstructures that sustain mechanical strength even after heating to 1,000 °C. Consequently, optimized mixtures (15%–20% MMT @ 800 °C) exhibit superior strength, chemical stability, and microstructural coherence compared with control concretes. The synergy between thermal activation, pozzolanic

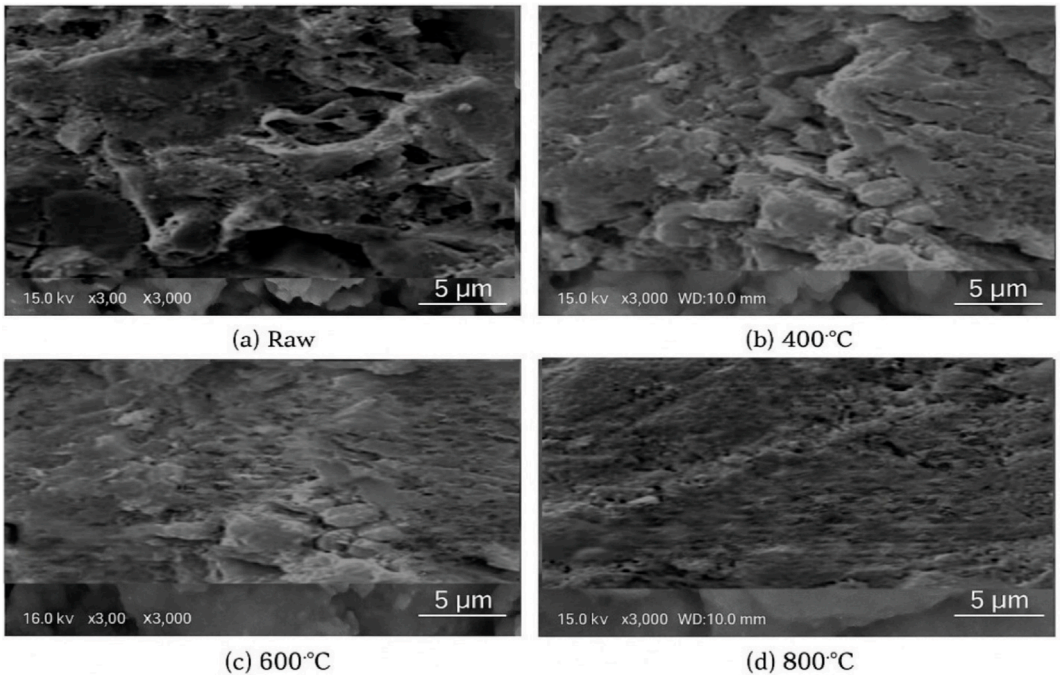

FIGURE 3
SEM images of montmorillonite: **(a)** raw, **(b)** calcined at 400 °C, **(c)** calcined at 600 °C, and **(d)** calcined at 800 °C, showing morphological transformation and increased densification with temperature.

reactivity, and microstructural refinement establishes calcined montmorillonite as a multifunctional, sustainable supplementary cementitious material that enhances both performance and environmental efficiency in advanced eco-concretes.

3.7 Analysis of variance (ANOVA)

Two-way analysis of variance (ANOVA) was conducted to quantitatively assess the individual and combined effects of calcination temperature (T) and replacement level (R) on the mechanical and durability properties of coffee biochar concrete, as summarized in Table 6. The objective of this analysis was not only to determine statistical significance, but also to identify the dominant controlling factors and to relate statistical outcomes to the underlying physicochemical mechanisms observed through XRD, FTIR, and SEM analyses (Mahmood et al., 2024).

For compressive strength, calcination temperature exhibited a very high F-value ($F = 155.35$) with an extremely low p-value ($p < 0.00001$), far exceeding the critical F-value. This clearly indicates that temperature is the dominant parameter controlling compressive strength development. The statistical dominance of temperature reflects the decisive role of thermal activation in transforming montmorillonite from a crystalline to an amorphous aluminosilicate phase, thereby enhancing pozzolanic reactivity and secondary gel formation. The replacement level also showed a statistically significant effect ($F = 21.66$, $p = 0.0018$), though its influence was markedly lower than that of temperature. This indicates that while dosage contributes to strength development, its effectiveness is contingent upon the activation state of the montmorillonite. The significant interaction term ($T \times R$, $p < 0.05$) further confirms that the influence of replacement level is not independent, but strongly dependent on calcination temperature, explaining why similar replacement levels yield different strength outcomes under different thermal conditions (Abdalla et al., 2023).

For tensile strength, an even stronger dependence on calcination temperature was observed, with an exceptionally high F-value ($F = 406.00$, $p = 2.57 \times 10^{-7}$). This result highlights the sensitivity of tensile behavior to microstructural cohesion and interfacial transition zone (ITZ) quality, both of which are strongly enhanced by amorphization and secondary hydration reactions. The replacement level also exhibited a highly significant effect ($F = 331.00$, $p = 7.25 \times 10^{-7}$), indicating that tensile strength is particularly responsive to optimized dosage due to its reliance on matrix continuity and crack resistance. The statistically significant interaction term confirms a synergistic effect, whereby optimal tensile performance is achieved only when adequate replacement levels are combined with sufficiently high calcination temperatures that maximize reactivity (Manju et al., 2024).

A similar statistical hierarchy was observed for flexural strength, where calcination temperature again dominated the response ($F = 278.54$, $p = 6.91 \times 10^{-7}$). This finding indicates that thermal activation plays a crucial role in improving flexural capacity by densifying the matrix, refining the pore structure, and enhancing crack-bridging mechanisms. The replacement level also showed a significant influence ($F = 58.33$, $p = 1.94 \times 10^{-4}$), suggesting that appropriate dosage enhances flexural behavior by improving stress transfer across microcracks. The significant interaction effect confirms that flexural performance benefits most from a balanced combination of activation temperature and replacement level rather than from either factor alone.

The ANOVA results for durability-related properties further reinforce the dominant role of calcination temperature. For mass loss in 10% NaCl, calcination temperature exhibited a high F-value ($F = 118.41$, $p = 3.15 \times 10^{-5}$), demonstrating that thermal activation significantly reduces chloride ingress and associated degradation. This statistical outcome aligns with SEM observations of pore refinement and reduced pore connectivity at higher calcination temperatures. The replacement level also contributed significantly ($F = 36.84$, $p = 5.33 \times 10^{-4}$), indicating that increased dosage enhances resistance to chloride penetration by further densifying the microstructure. The significant interaction term confirms that chloride resistance is maximized through a synergistic combination of activation and dosage optimization.

For mass loss in 5% HCl, calcination temperature showed an even stronger statistical influence ($F = 206.97$, $p = 1.91 \times 10^{-6}$), underscoring its critical role in acid resistance. This behavior reflects the enhanced consumption of calcium hydroxide and the formation of chemically stable secondary gels, which reduce the availability of acid-soluble phases. Replacement level remained statistically significant ($F = 49.46$, $p = 1.87 \times 10^{-4}$), while the significant interaction term indicates a strong synergistic effect under acidic conditions, where optimized dosage amplifies the benefits of thermal activation as shown in Table 7.

Similarly, for mass loss in 5% HNO_3, calcination temperature was identified as the primary durability-controlling factor, while the replacement level ($F = 133.36$, $p = 1.06 \times 10^{-5}$) and interaction effects were also statistically significant. The high sensitivity of nitric acid resistance to both factors reflects the aggressive nature of nitric acid and the importance of both reduced portlandite content and refined pore structure in mitigating degradation. The interaction effect further confirms that long-term chemical stability is optimized only when appropriate replacement levels are combined with effective thermal activation (Mohammed and Nahazanan, 2023).

Overall, the ANOVA results clearly establish a consistent hierarchy of influence across all investigated properties: calcination temperature > replacement level > interaction effect, with calcination temperature emerging as the primary controlling parameter. The repeated statistical significance of the interaction term across mechanical and durability responses confirms that the performance of coffee biochar concrete is governed by a coupled mechanism, rather than by independent effects of temperature or dosage. These findings provide strong quantitative validation of the microstructural observations obtained from XRD, FTIR, and SEM analyses, which demonstrated progressive amorphization, calcium hydroxide consumption, pore refinement, and ITZ densification. Consequently, the ANOVA analysis not only confirms statistical significance, but also provides a robust numerical framework linking material chemistry, microstructure, and macroscopic performance.

3.8 Physical and mechanical properties

The physical and mechanical characteristics of montmorillonite-blended concrete were strongly influenced by calcination temperature (T), replacement level (R), and their interaction (T × R). ANOVA revealed that each factor had a statistically significant effect ($p < 0.05$) on the studied parameters, including bulk density, compressive strength, tensile strength, flexural strength, and Vickers hardness. The calcination temperature consistently produced the highest F-values, highlighting its dominant role in dictating the reactivity of montmorillonite and the degree of pozzolanic activity. The replacement level, on the other hand, controlled the amount of reactive amorphous phase available for secondary hydration reactions, while the interaction term (T × R) amplified the synergistic response of the system, confirming that the mechanical improvements arise from a coupled thermo-chemical mechanism rather than isolated material variations (Abdalla et al., 2023).

3.8.1 Bulk density

The results show that incorporating both calcined and raw montmorillonite in concrete reduces the fresh bulk density compared to the control mixture. A significant reduction in fresh bulk density is observed as the montmorillonite content increases from 5% to 20%. This is primarily due to the lower specific gravity of montmorillonite compared to cement, which leads to a reduction in the overall mass per unit volume of the concrete mixture.

This reduction in fresh bulk density can be attributed to several factors. Montmorillonite has a layered silicate structure and high surface area, which increases the water demand of the mix, thereby affecting its workability and compaction (Mokhtari, 2019). Additionally, the finer particle size of montmorillonite compared to cement contributes to a higher volume of paste with lower mass, leading to a lower density (Yusuf, 2024; Andreola et al., 2019; Chantal, 2020; Chung et al., 2021; Fode et al., 2024a). The pozzolanic reactivity of calcined montmorillonite allows it to partially replace cement while contributing to the formation of additional calcium silicate hydrate (C–S–H) gel, although this primarily influences long-term strength rather than fresh density as explained in Figure 4.

The reduction in fresh bulk density may also result from decreased water content at higher montmorillonite replacement levels, as montmorillonite absorbs more water due to its high specific surface area (Pinto et al., 2023). This alters the mix water-to-binder ratio and can slightly reduce compaction efficiency. Moreover, increasing the calcination temperature of montmorillonite further reduces the fresh bulk density of the concrete. This is due to the breakdown of montmorillonite structure at higher temperatures, resulting in finer, more porous particles that replace the denser cement particles and occupy more volume with less mass.

3.8.2 Compressive strength

Compressive strength exhibited a clear upward trend with increasing calcination temperature and moderate replacement levels. The ANOVA indicated that temperature ($F = 155.35$; $p < 0.00001$) was the most influential factor, followed by replacement level ($F = 21.66$; $p = 0.0018$), with the interaction term also significant ($p < 0.05$). The control mix achieved ≈46 MPa at 28 days, whereas mixes with 15%–20% MMT calcined at 600 °C–800 °C reached 50–52 MPa, a gain of approximately 10%–15%. This increase is attributed to the high pozzolanic activity of the amorphous aluminosilicate phases generated during calcination. At 600 °C–800 °C, the structural dehydroxylation of montmorillonite breaks Al–OH and Si–O–H bonds, producing reactive SiO_2 and

10.3389/fmats.2026.1755011

TABLE 7 Analysis of variance (ANOVA).

Property	Source of variation	F-value	p-Value	F (crit)	Significance	Interpretation
Compressive strength (MPa)	Calcination temperature (T)	155.35	<0.00001	4.757	Significant ($p < 0.05$)	Temperature dominates; enhances reactivity and strength
	Replacement level (R)	21.66	0.0018	5.143	Significant ($p < 0.05$)	Moderate R boosts pozzolanic reaction
	Interaction (T × R)	—	$p < 0.05$	—	Significant ($p < 0.05$)	Synergistic temperature–replacement effect
Tensile strength (MPa)	Calcination temperature (T)	406.00	2.57×10^{-7}	4.757	Significant ($p < 0.05$)	Thermal activation drives amorphization and cohesion
	Replacement level (R)	331.00	7.25×10^{-7}	5.143	Significant ($p < 0.05$)	Dosage strongly affects tensile gain
	Interaction (T × R)	—	$p < 0.05$	—	Significant ($p < 0.05$)	Positive interaction strengthens ITZ bonding
Flexural strength (MPa)	Calcination temperature (T)	278.54	6.91×10^{-7}	4.757	Significant ($p < 0.05$)	Temperature densifies microstructure; improves flexural capacity
	Replacement level (R)	58.33	1.94×10^{-4}	5.143	Significant ($p < 0.05$)	Optimum R enhances crack bridging
	Interaction (T × R)	—	$p < 0.05$	—	Significant ($p < 0.05$)	Synergy between activation and dosage
Mass loss in 10% NaCl (%)	Calcination temperature (T)	118.41	3.15×10^{-5}	4.757	Significant ($p < 0.05$)	Temperature reduces chloride permeability
	Replacement level (R)	36.84	5.33×10^{-4}	5.143	Significant ($p < 0.05$)	Higher R lowers NaCl penetration
	Interaction (T × R)	—	$p < 0.05$	—	Significant ($p < 0.05$)	Interaction enhances salt-ion resistance
Mass loss in 5% HCl (%)	Calcination temperature (T)	206.97	1.91×10^{-6}	4.757	Significant ($p < 0.05$)	Temperature greatly improves acid durability
	Replacement level (R)	49.46	1.87×10^{-4}	5.143	Significant ($p < 0.05$)	Higher R reduces acid solubility
	Interaction (T × R)	—	$p < 0.05$	—	Significant ($p < 0.05$)	Strong synergistic effect under HCl exposure
Mass loss in 5% HNO_3 (%)	Calcination temperature (T)	441.45	2.00×10^{-7}	4.757	Significant ($p < 0.05$)	Temperature is dominant durability factor
	Replacement level (R)	133.36	1.06×10^{-5}	5.143	Significant ($p < 0.05$)	Replacement enhances acid attack resistance
	Interaction (T × R)	—	$p < 0.05$	—	Significant ($p < 0.05$)	Interaction optimizes long-term stability

Al_2O_3 components. These amorphous species react readily with portlandite ($Ca(OH)_2$) liberated during cement hydration, forming additional C–S–H, C–A–S–H, and C–A–H phases. The formation of these gels refines the pore structure, strengthens the interfacial transition zone (ITZ), and increases the load-bearing capacity as explained in Figure 5.

XRD and FTIR results support this mechanism, showing the disappearance of crystalline montmorillonite peaks and the broadening of amorphous humps at $2\theta = 27°–32°$, along with a shift of the Si–O stretching band to ≈1,040 cm^{-1}. Interestingly, curing age had a smaller F-value compared with temperature, indicating that the strength plateaued by 56 days, consistent with near-complete pozzolanic reaction (Abdalla et al., 2023). The observed strength enhancement is thus governed by chemical reactivity rather than extended hydration time (Mohammed and Nahazanan, 2023).

3.8.3 Tensile and flexural strengths

Both tensile and flexural strengths followed the same trend as compressive strength but displayed stronger statistical sensitivity to the interaction term (T × R). The ANOVA reported F-values of 406.00 for tensile and 278.54 for flexural strength, each with p-values below 10^{-6}, confirming that these differences are statistically robust. Tensile strength improved by 25%–30% at optimum conditions (15%–20% MMT, 800 °C), while flexural strength rose by a comparable margin. The increase in tensile strength is associated with improved interfacial transition zone ITZ bonding and the reduction of micro crack initiation sites. The pozzolanic gel fills microvoids, binding aggregates and creating a more cohesive matrix capable of resisting tension-induced stress localization. SEM micrographs clearly showed continuous C–S–H gel networks

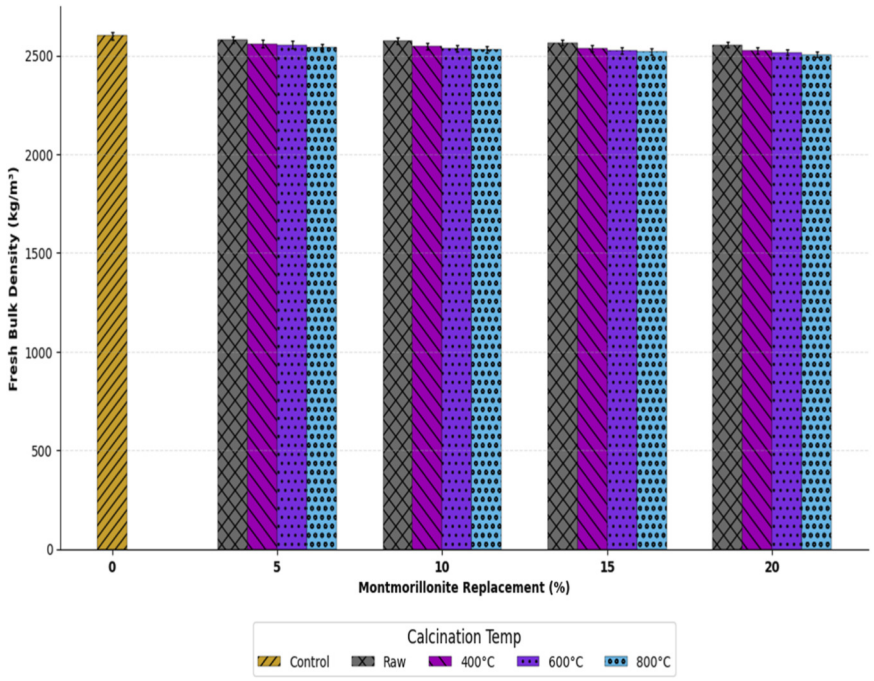

FIGURE 4
Bulk density.

surrounding aggregate surfaces, confirming densification of the interfacial transition zone ITZ (Qin et al., 2022).

Flexural strength, a composite indicator of tensile and compressive performance, responded strongly to both calcination and replacement. At 600 °C–800 °C, the montmorillonite's high reactivity enhanced matrix continuity and improved crack propagation resistance under bending As explained in Figures 6, 7. The mixes containing unclaimed or low-temperature MMT (≤400 °C) performed poorly, exhibiting lower strength due to incomplete dehydroxylation and persistence of weak, laminar clay platelets that inhibited cement hydration. The coupling between thermal activation and compositional dosage amplified mechanical synergy: the same 15% replacement produced only modest improvement at 300 °C but delivered a twofold strength increase at 800 °C (Abdalla et al., 2023).

3.8.4 Vickers Hardness

The Vickers hardness results paralleled the tensile and flexural trends, acting as a micro-indicator of densification and surface strength as explained in Figure 8. Hardness increased consistently with calcination temperature and moderate replacement levels, peaking at 15% MMT calcined at 800 °C. The ANOVA indicated temperature as a dominant factor ($F \approx 120$; $p < 0.001$). The improvement arises from the densification of near-surface layers by tightly bonded secondary gels that inhibit surface indentation. The hardness enhancement is not a superficial phenomenon; it reflects genuine microstructural consolidation. Under optimal conditions, the surface becomes rich in C–S–H and C–A–S–H gels with limited porosity, reducing indentation depth and enhancing scratch resistance. Conversely, concretes with raw or low-temperature MMT displayed lower hardness values due to residual crystalline impurities that acted as local weaknesses.

FTIR results confirmed this trend, as hydroxyl peaks around 3,440 cm^{-1} (O–H stretching) diminished with temperature, while Si–O and Al–O peaks broadened, indicating increased polymerization of the gel phase. This transformation correlates directly with the statistical outcomes—higher temperature yields greater amorphization, more cohesive bonding, and correspondingly higher hardness (Shaji and Divya, 2024).

3.8.5 Integrated mechanistic interpretation

The collective results from bulk density, strength, and hardness analyses establish a coherent mechanism linking statistical, experimental, and microstructural findings: calcination temperature determines the structural activation of montmorillonite, transforming it from a layered crystalline clay to a reactive amorphous phase; replacement level defines the quantity of reactive surfaces available to participate in pozzolanic reaction; and their interaction maximizes synergy. At optimal conditions—600 °C–800 °C calcination and 15%–20% replacement—the microstructure achieves the ideal balance between reactivity and compaction. SEM–EDS analyses revealed reduced Ca/Si ratios (from ≈2.1 to ≈1.6) and uniform C–S–H gel dispersion, while FTIR confirmed the progressive shift of Si–O–Si stretching bands and the suppression of hydroxyl vibrations (Shaji and Divya, 2024). In engineering terms, these results indicate that temperature is not only a variable in processing

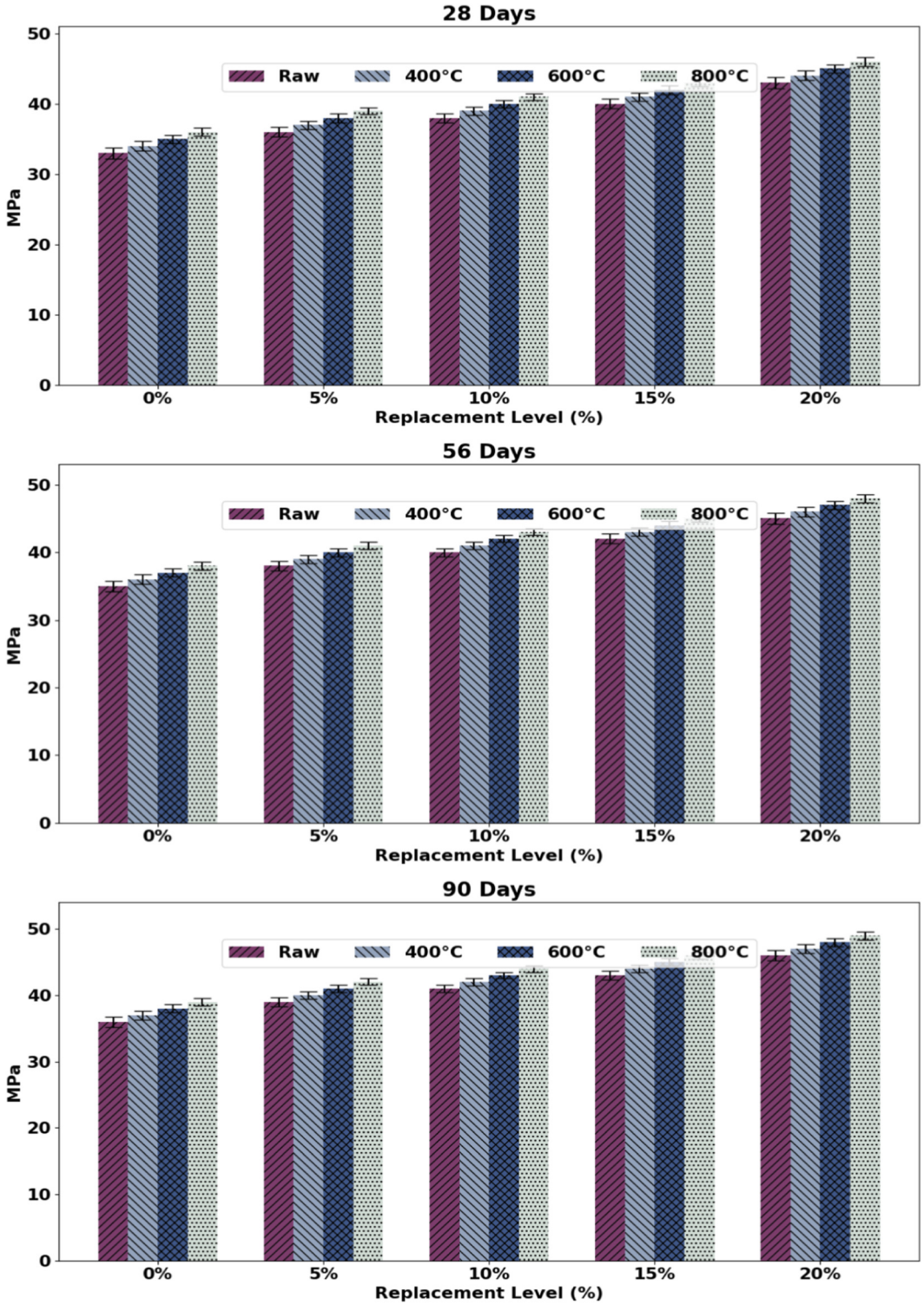

FIGURE 5
Compressive strength.

but a performance determinant. Its effect propagates through the hydration–pozzolanic cycle, modifying gel chemistry, pore topology, and mechanical response. Collectively, the results affirm that thermally activated montmorillonite behaves as a sustainable high-performance supplementary cementitious material (SCM) that enhances strength, hardness, and density while promoting a more durable, environmentally responsible cement composite.

10.3389/fmats.2026.1755011

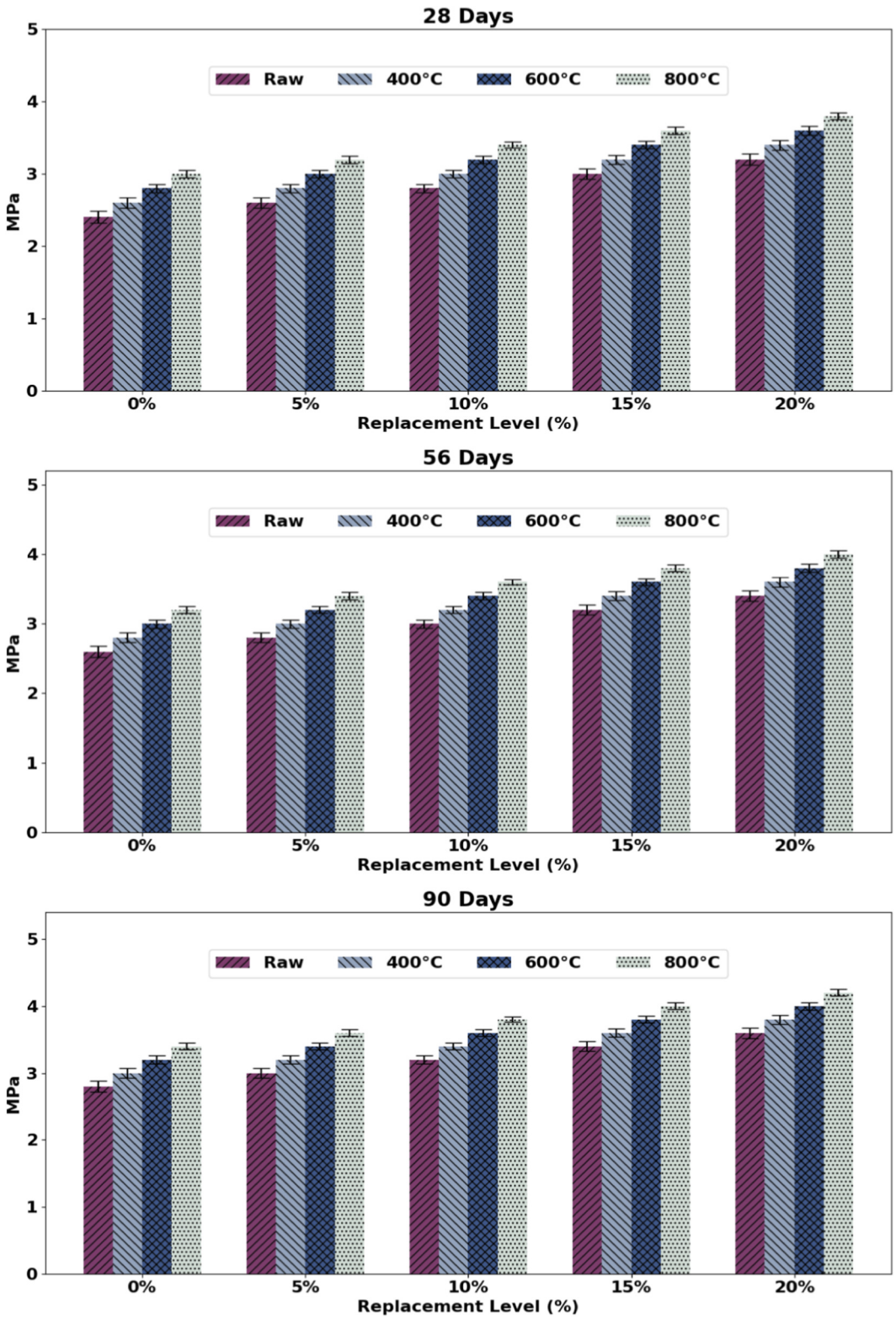

FIGURE 6
Tensile strength.

10.3389/fmats.2026.1755011

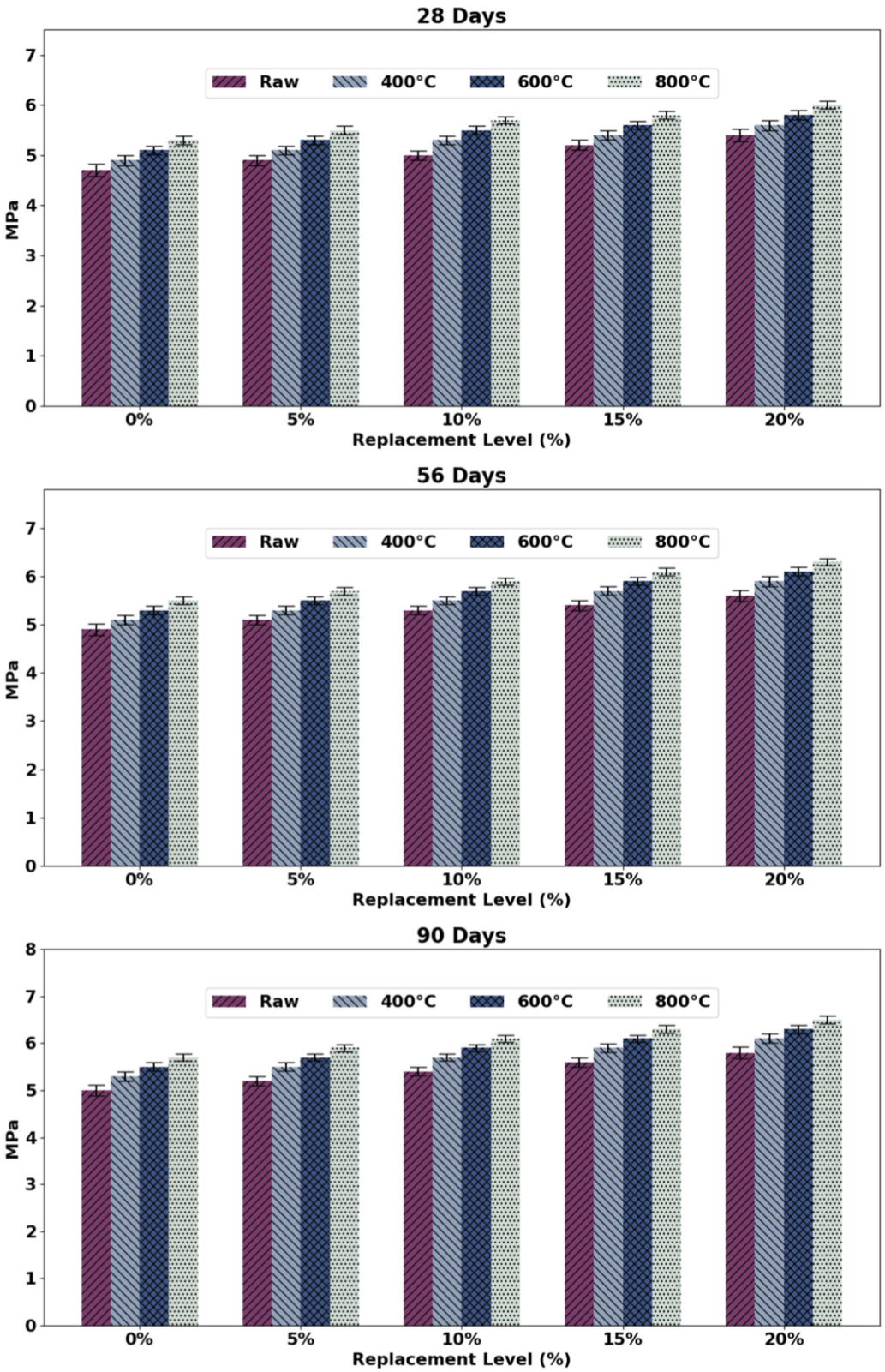

FIGURE 7
Flexural strength.

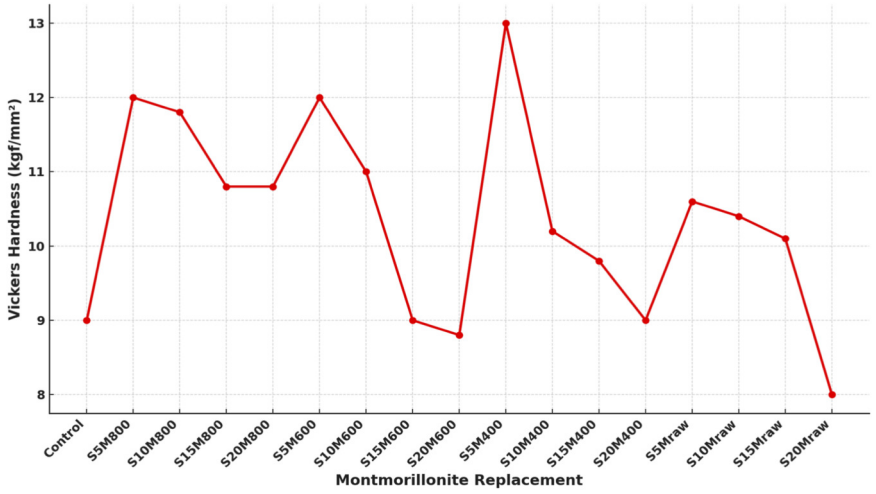

FIGURE 8
Vickers hardness.

3.9 Chemical attack resistance

The chemical resistance of montmorillonite-blended concrete is a crucial indicator of its long-term durability under aggressive environmental exposure. In this study, chemical durability was evaluated through mass-loss analyses after immersion in 5% HCl, 5% HNO_3, and 10% NaCl solutions for periods up to 90 days. The test results clearly reveal that the extent of deterioration was highly dependent on calcination temperature (T), replacement level (R), and their interaction (T × R). Statistical analysis (two-way ANOVA) confirmed the strong significance of all three parameters ($p < 0.05$), with calcination temperature producing the highest F-values, thereby governing the durability response across all environments. At optimum conditions—15%–20% MMT calcined at 600–800 °C—the mean mass-loss reduction reached 70%–85% compared with the control concrete. These results prove that thermal activation of montmorillonite profoundly improves its pozzolanic efficiency, leading to the formation of dense, chemically stable matrices capable of resisting both acid dissolution and chloride ingress (Yusuf, 2024).

3.9.1 Mass loss in 5% HCl solution

Hydrochloric acid attack, representing a strong leaching environment, resulted in significant degradation in the control sample but minimal mass loss in the thermally activated mixes. The control mix recorded a mass loss of approximately 3.6% after 28 days, whereas concrete incorporating 20% MMT calcined at 800 °C lost only 0.6%–0.8% of its mass. The statistical analysis confirmed that calcination temperature was the most influential variable ($F = 206.97$, $p = 1.9 \times 10^{-6}$). Mechanistically, HCl readily reacts with $Ca(OH)_2$ and weakly bound C–S–H phases, forming soluble calcium chloride and leaving a porous, friable surface. However, in the optimized MMT-based concrete, the portlandite content was drastically reduced due to vigorous pozzolanic reactions that produced C–A–S–H gels with lower Ca/Si ratios and higher polymerization. SEM images of control specimens showed extensive surface dissolution, micro-pitting, and decalcification layers, while those of thermally activated samples appeared smooth, dense, and free from major defects (Shaji and Divya, 2024).

EDS analyses corroborated this by revealing a decrease in the Ca/Si ratio from ≈2.1 (control) to ≈1.6 (800 °C MMT), evidencing near-complete consumption of portlandite. FTIR spectra further supported these observations. The control concrete exhibited a marked drop in the O–H stretching band near 3,440 cm^{-1} after acid exposure, indicating severe $Ca(OH)_2$ leaching, whereas the activated MMT mixes preserved strong Si–O–Si and Si–O–Al bands around 1,040 cm^{-1}, reflecting the chemical resilience of the amorphous aluminosilicate matrix as illustrated in Figure 9.

3.9.2 Mass loss in 5% HNO_3 solution

Nitric acid, being more oxidizing and aggressive than hydrochloric acid, caused higher degradation in all mixes; yet the calcined MMT concretes still displayed remarkable resistance. The ANOVA produced the highest F-value among all tests ($F = 441.45$; $p = 2 \times 10^{-7}$), highlighting the exceptional dominance of temperature. Mass loss decreased from ≈3.2% (control) to ≈0.4% at 15%–20% replacement and 800 °C calcination, confirming an eightfold improvement in chemical stability. The enhanced performance in nitric acid can be attributed to the polymerization of aluminosilicate chains within the C–A–S–H gel, which stabilizes the structure against nitric-acid attack. FTIR spectra of these samples showed diminished hydroxyl bands near 3,440 cm^{-1} and reinforced Si–O–Al linkages near 1,010 cm^{-1}, confirming stronger cross-linking and reduced solubility. The formation of a thin, stable silica gel layer at the surface acts as a protective barrier that slows further leaching As illustrated in Figure 10.

SEM micrographs revealed that the control specimen developed a rough, honeycomb-like surface and large pores after 28 days in HNO_3, while the optimized specimen retained a compact and continuous matrix. The difference in damage depth was

10.3389/fmats.2026.1755011

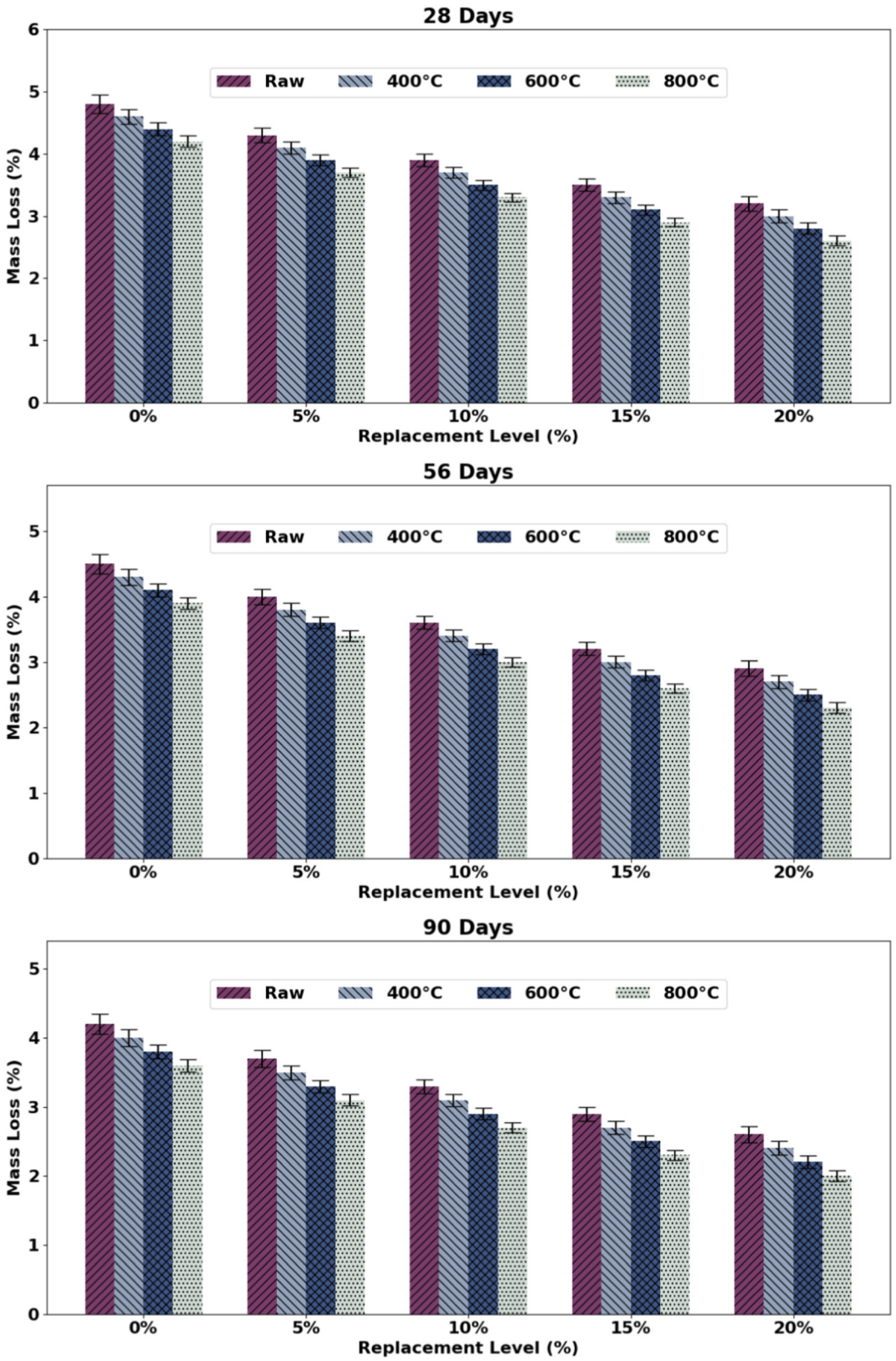

FIGURE 9
Mass loss in 5% HCl solution.

10.3389/fmats.2026.1755011

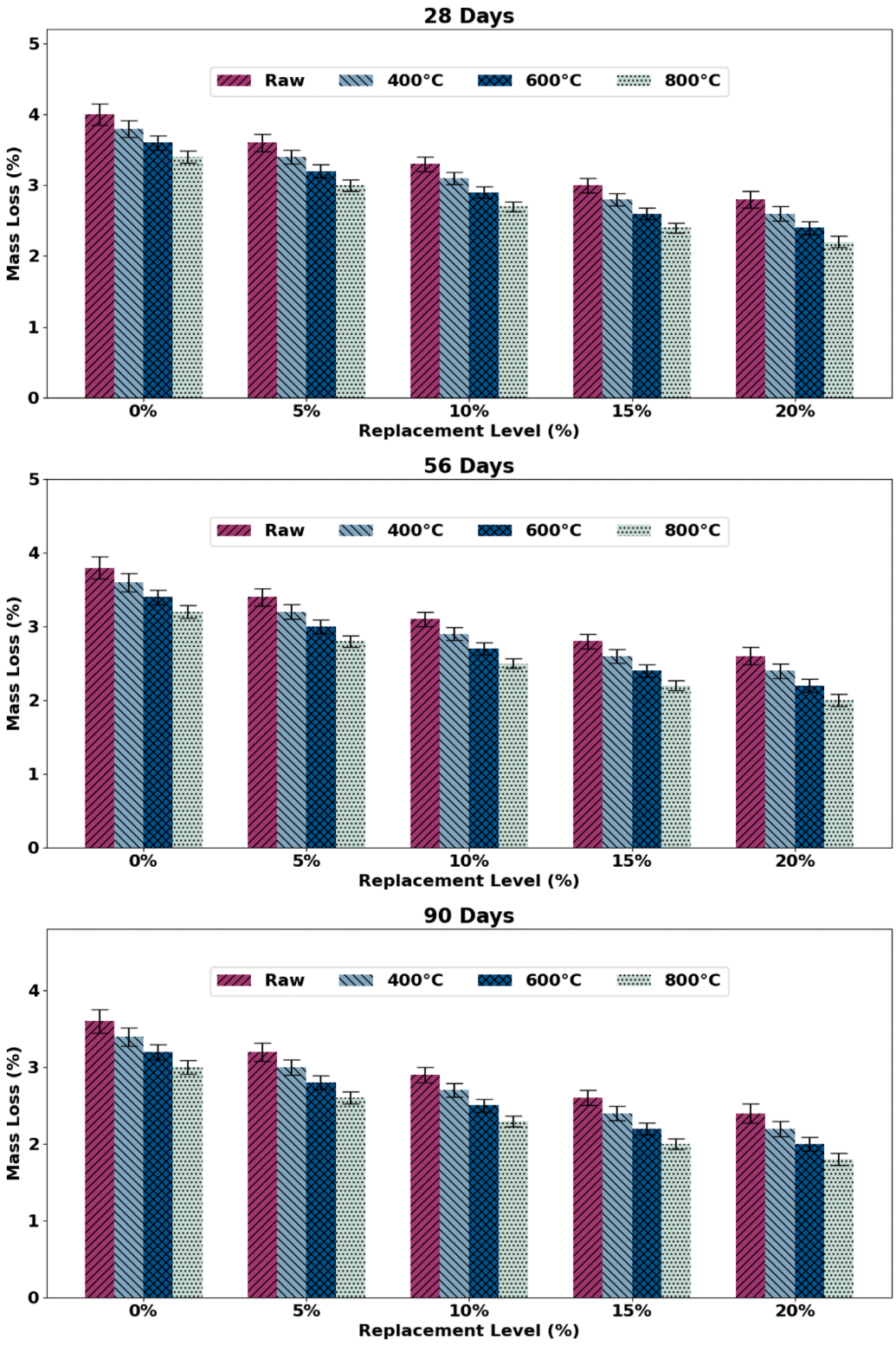

FIGURE 10
Mass loss in 5% HNO_3 solution.

approximately 1.5–2 mm (control) versus <0.3 mm (optimized), confirming the correlation between microstructure and mass-loss data.

3.9.3 Mass loss in 10% NaCl solution

Chloride exposure, while less chemically aggressive than acid attack, plays a pivotal role in corrosion initiation and long-term durability. The ANOVA yielded F = 118.41 ($p = 3.15 \times 10^{-5}$) for temperature, confirming strong significance As illustrated in Figure 12. Mass-loss values decreased from ≈2.8% (control) to ≈0.4% (15% MMT at 800 °C). The optimized specimens maintained their integrity with no visible cracks or efflorescence even after 90 days, unlike the control, which exhibited white salt deposits and micro-scaling. The reduction in chloride-induced deterioration results from both physical densification and chemical ion exchange. Calcined MMT contains exchangeable Na^+, Ca^{2+}, and Al^{3+} sites that can bind Cl^- ions within the interlayer or gel network, thereby lowering the concentration of free chlorides in pore solution as illustrated in Figure 11. MIP data showed a reduction in total porosity from 16.3% (control) to 9.2% (optimized mix), and the threshold pore diameter decreased from 0.053 μm to 0.021 μm, directly correlating with decreased ionic permeability (Andreola et al., 2019).

3.9.4 Effects of Different Hazardous Environments by Residual Analysis

As illustrated in Figure 12, the residual results from the compressive strength tests reveal significant differences for concrete mortar cubes cured for 90 days in various environments, including 5% hydrochloric acid, 5% nitric acid, normal water, and under elevated temperatures of 200 °C for 2 h. The findings depicted in Figure 14 demonstrate distinct fracture patterns among the samples, highlighting the impact of each curing environment on the structural integrity of the concrete.

Notably, the concrete mortar cubes cured in acid exhibit a perpendicular fracture pattern, indicating a different failure mechanism compared to those cured in water or subjected to elevated temperatures, which display a V-shaped fracture pattern. This variation in fracture characteristics can be attributed to the differing locations of maximum stress within each sample (Manju et al., 2024). In the acid-cured samples, the corrosive nature of the acids primarily affects the external surfaces, leading to concentrated stress in the middle of the concrete cubes. As a result, fractures occur perpendicular to the applied loads, reflecting the weakness induced by acid exposure (Saraber, 2017; Haque and Armeniades, 1986; Hepautwa and Jande, 2025; Jafari and Sadeghian, 2025; Khand and Nomana, 2019; Wu, 2025).

In contrast, the concrete mortar cubes cured in normal water and those exposed to elevated temperatures experience a more uniform stress distribution, resulting in V-shaped fractures. This pattern signifies that the structural integrity of these samples is maintained more effectively, allowing for load-bearing capabilities to be retained across a broader area. The elevated temperature curing, in particular, may enhance the hydration process, leading to denser microstructures that can better withstand stress and resist cracking.

These observations underscore the importance of understanding how different hazardous environments influence the mechanical properties of concrete. The distinct fracture patterns not only provide insight into material behavior under various conditions but also suggest practical implications for construction practices, especially in environments where exposure to acidic substances or extreme temperatures is a concern.

Overall, the results emphasize the need for careful consideration of material selection and curing methods to ensure the durability and performance of concrete motor structures in challenging environments. By understanding how different curing conditions affect material properties, engineers and architects can make informed decisions that enhance the longevity and safety of concrete infrastructure.

3.10 Effect of high temperature

The residual mechanical performance of montmorillonite-blended concrete exposed to high temperatures was examined to evaluate thermal stability and fire resistance. Specimens were heated to 200 °C, 400 °C, 600 °C, 800 °C, and 1,000 °C, then cooled to ambient temperature before testing. The results demonstrate that both calcination temperature (T) of the montmorillonite additive and replacement level (R) significantly influenced residual strength, with their interaction (T × R) also statistically significant ($p < 0.05$). ANOVA indicated that the effect of high temperature was strongly correlated with initial activation conditions: concretes containing calcined MMT at 600 °C–800 °C and 15%–20% replacement exhibited the highest residual strength retention, while uncalcined or low-temperature MMT mixes suffered rapid deterioration beyond 400 °C.

The results from the 2-h elevated temperature test at 200 °C are presented in Figure 14. In this study, the substitution of raw montmorillonite demonstrates the lowest mechanical strength when subjected to high temperatures, especially in comparison to both the control samples and those that incorporate calcined montmorillonite. This diminished strength is primarily attributed to the inherent properties of raw montmorillonite, which tends to exist in a consolidated form, rendering it less reactive (Mohammed and Nahazanan, 2023). This lack of reactivity is crucial, as it limits the material's ability to interact effectively with other components in the matrix, resulting in suboptimal performance under thermal stress.

Moreover, the analysis reveals that the mass loss experienced by raw montmorillonite is significantly higher. This mass loss is an important factor to consider, as it indicates the material's susceptibility to thermal degradation. As the calcination temperature increases, however, this mass loss tends to decrease. This trend can be explained by the fact that higher calcination temperatures enhance the reactivity of montmorillonite. During calcination, the material undergoes structural transformations that promote the formation of an amorphous phase (Shaji and Divya, 2024). This amorphous phase is crucial because it increases the volume of hydrated phases within the material, which contributes to improved densification and agglomeration of the binder matrix.

The enhancement of these properties is particularly significant when considering the application of montmorillonite in cement composite materials at elevated temperatures. As the calcination

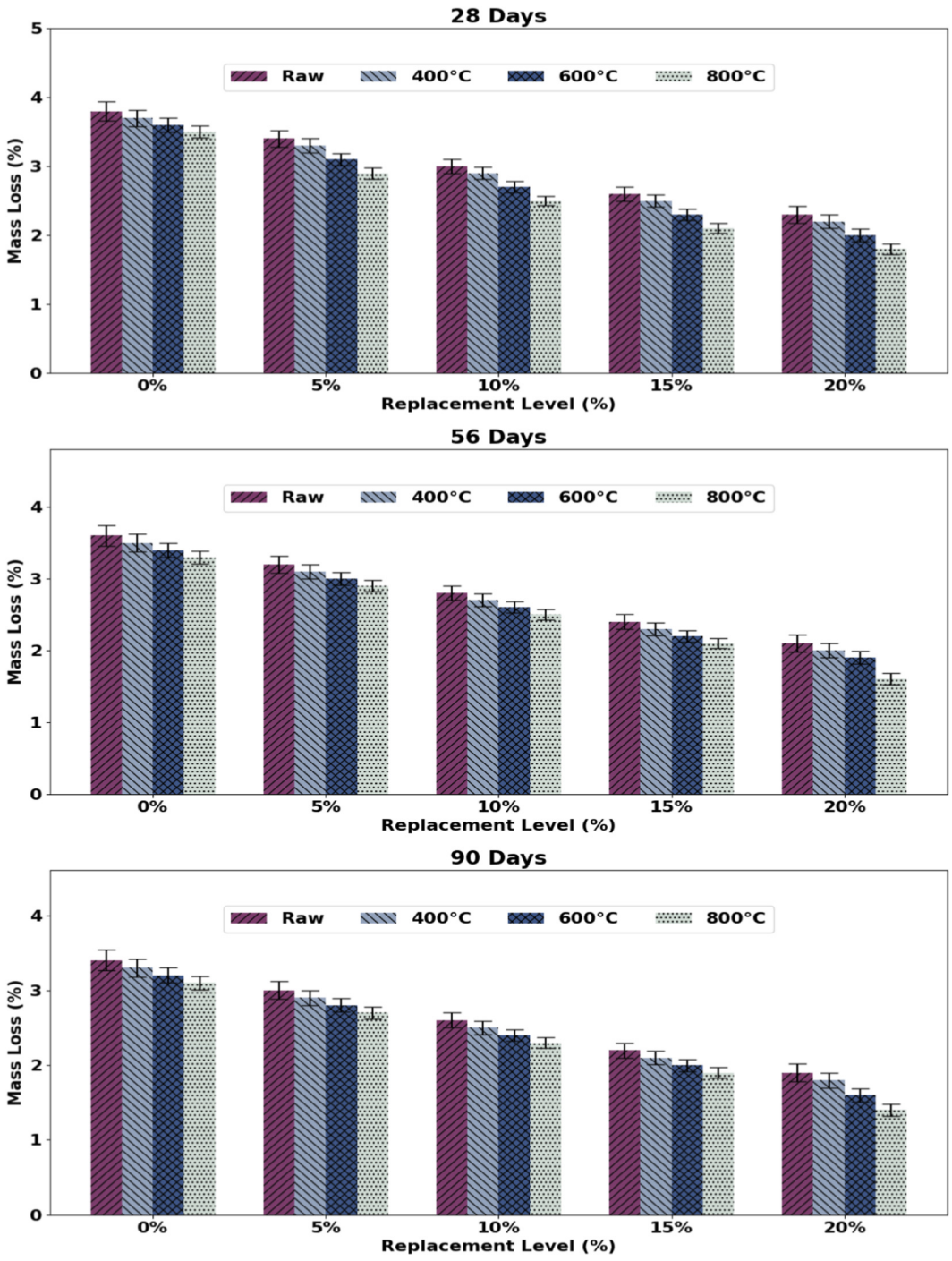

FIGURE 11
Mass loss in 10% NaCl solution.

temperature is raised from 400 °C to 800 °C, a marked improvement in strength is observed at 200 °C. This is a critical finding for construction and materials engineering, as it suggests that the careful selection of calcination conditions can lead to stronger and more resilient materials as explained in Figure 13.

Furthermore, all samples that utilize montmorillonite calcined at 800 °C exhibit a superior ability to withstand elevated temperatures compared to those with lower calcination temperatures or raw montmorillonite. This enhanced resistance is vital for applications in environments subject to high thermal stress, making calcined montmorillonite a favorable choice in the development of high-performance cementitious materials.

Overall, the findings emphasize the importance of both the reactivity and structural properties of montmorillonite

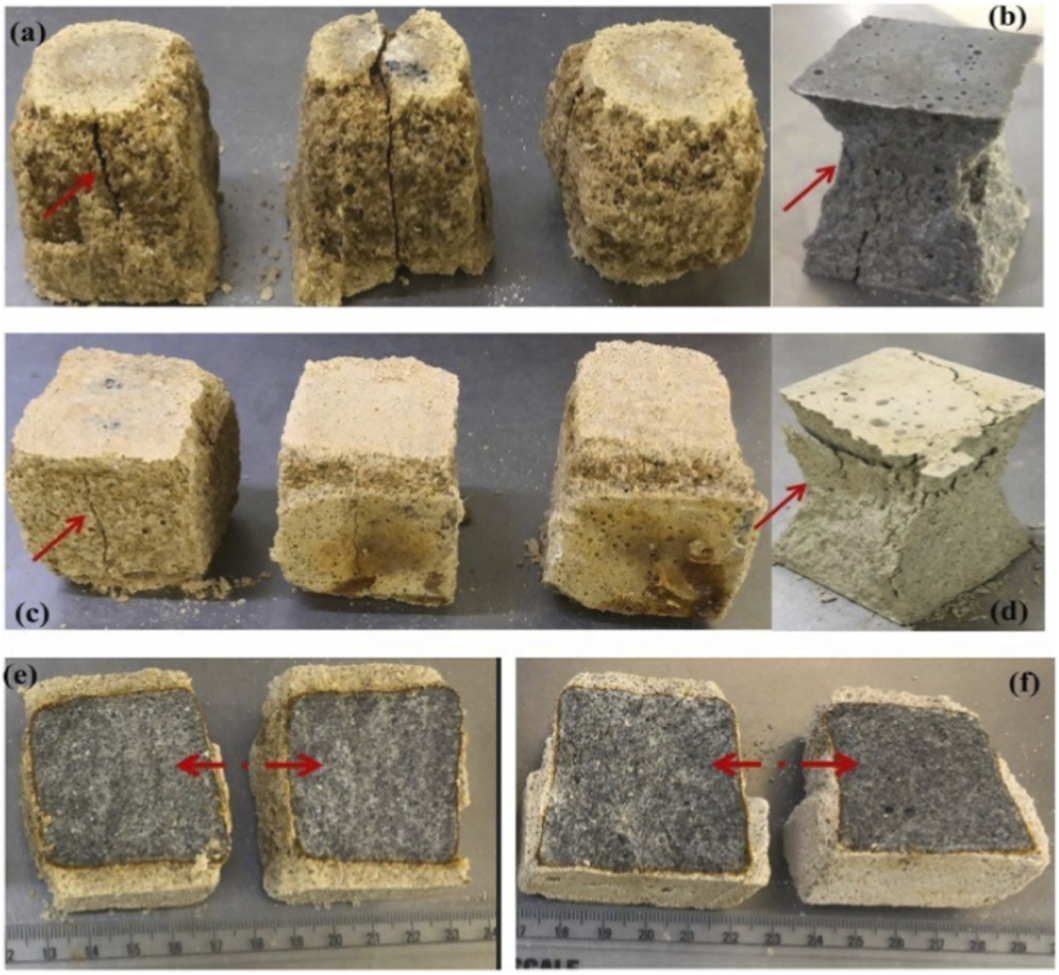

FIGURE 12
Residual and failure characteristics of specimens under different exposure conditions: **(a–f)** Representative images showing cracking, interface separation, and structural degradation.

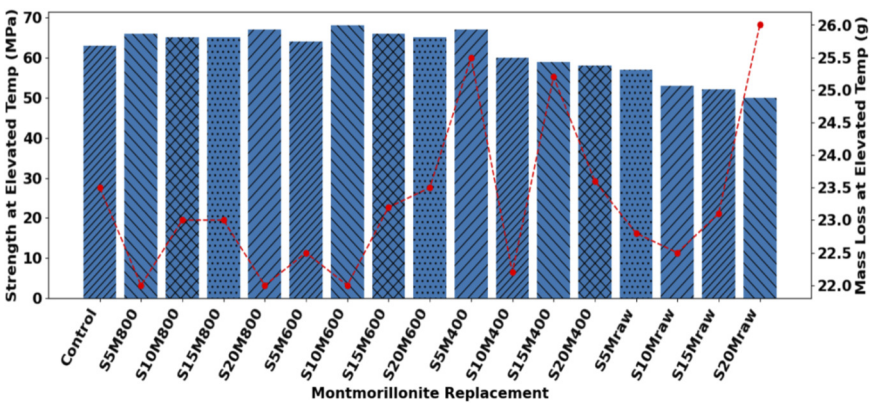

FIGURE 13
Effect of temperature.

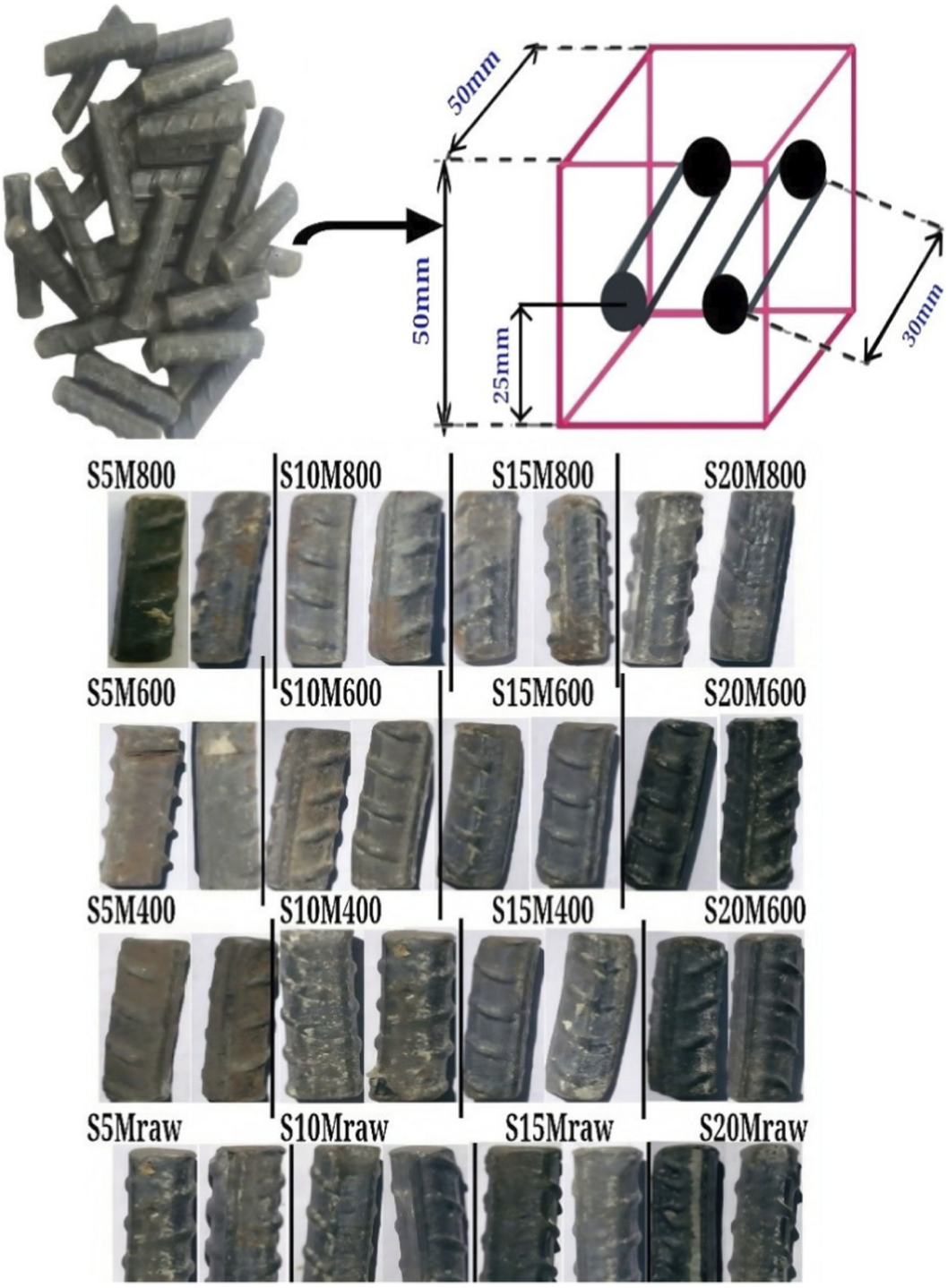

FIGURE 14
Effects of different hazardous environments by residual analysis.

in determining its effectiveness as a component in cement composites, particularly under conditions of thermal stress. Understanding these relationships can guide future research and applications, ensuring that the materials developed are both durable and efficient.

3.11 Corrosion analysis

The corrosion behavior of embedded steel reinforcement was examined after 90 days of exposure to a 10% NaCl solution. The evaluation was based on visual inspection of extracted steel bars

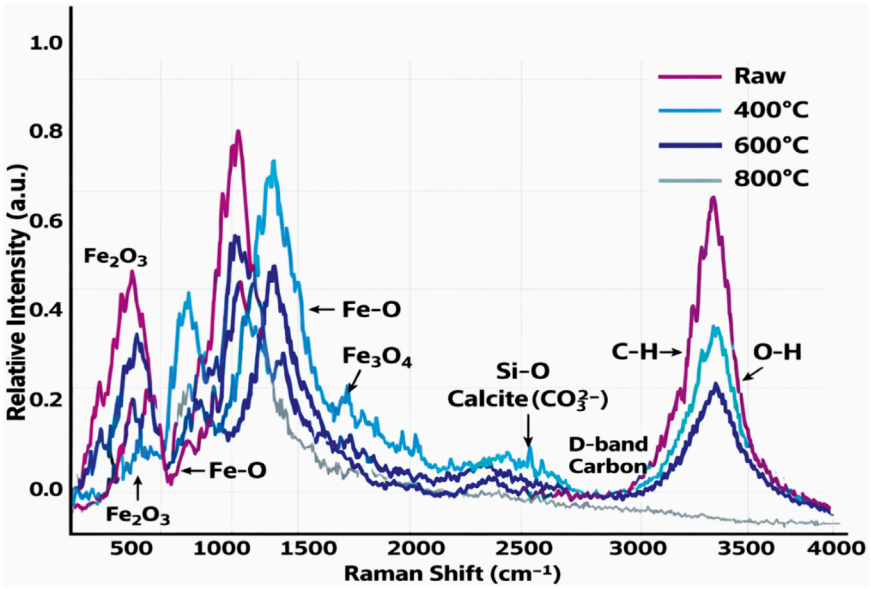

FIGURE 15
Raman spectra of montmorillonite calcined at 400 °C, 600 °C, and 800 °C showing the disappearance of Fe–O bands and hydroxyl peaks associated with reduced iron oxidation and improved corrosion resistance.

and microstructural analysis of the surrounding mortar matrix using scanning electron microscopy (SEM) and Raman spectroscopy. The purpose of this assessment was to investigate the influence of montmorillonite calcination temperature and replacement level on resistance to chloride-induced corrosion.

Visual examination revealed noticeable differences between the control specimen and mixtures containing calcined montmorillonite. The control sample exhibited visible rust formation, surface discoloration, and localized corrosion deposits along the steel surface. In contrast, specimens incorporating montmorillonite calcined at 600 °C–800 °C showed comparatively fewer corrosion products and improved surface condition. Representative images of the extracted reinforcement and corresponding SEM observations of the steel–mortar interface are presented in Figure 14 (Chantal, 2020).

Figure 15 Visual inspection of extracted steel bars and SEM images of the steel–mortar interfacial transition zone (ITZ) after 90 days of exposure to 10% NaCl solution.

SEM micrographs indicated that the control specimen possessed a relatively porous and heterogeneous interfacial transition zone (ITZ), with interconnected voids that may facilitate chloride penetration. Conversely, mortars containing calcined montmorillonite displayed a denser and more compact ITZ, characterized by reduced pore connectivity. This refinement is attributed to enhanced pozzolanic reaction and secondary gel formation resulting from thermal activation of montmorillonite, which contributes to matrix densification.

Raman spectroscopy analysis was conducted to identify corrosion-related iron oxide phases on the steel surface. The control specimen exhibited stronger spectral features corresponding to iron oxide compounds, whereas reduced peak intensities were observed in specimens incorporating calcined montmorillonite. The representative Raman spectra are shown in Figure 15 (Mohammed and Nahazanan, 2023).

It is important to clarify that the corrosion assessment performed in this study is qualitative. The interpretation of improved corrosion resistance is based on visual evidence, reduced apparent corrosion products, and microstructural densification of the matrix. No quantitative electrochemical measurements—such as half-cell potential (ASTM C876), corrosion current density, electrochemical impedance spectroscopy (EIS), or gravimetric mass loss of embedded steel—were conducted.

Therefore, the findings should be interpreted as indicative of enhanced corrosion resistance rather than conclusive quantitative proof. The observed improvement is inferred from reduced chloride accessibility and improved microstructural compactness associated with calcined montmorillonite incorporation (Chung et al., 2021; Fode et al., 2024a).

Future studies incorporating electrochemical monitoring and mass loss evaluation are recommended to provide quantitative validation of the corrosion mitigation potential suggested by the present qualitative observations.

4 Conclusion

This study evaluated the effects of raw and calcined montmorillonite (400 °C–800 °C) incorporated at 0%–20% replacement levels on the mechanical and durability performance of coffee ash concrete. The results demonstrate that calcination temperature is the dominant factor governing performance, while replacement level plays a secondary but statistically significant role.

Microstructural analyses (XRD, FTIR, and SEM) confirmed that progressive calcination from raw to 800 °C transforms montmorillonite from a crystalline layered structure into a highly reactive amorphous aluminosilicate phase. Calcination within the range of 600 °C–800 °C, combined with moderate replacement levels, promoted enhanced pozzolanic reactivity, secondary C–S–H/C–A–S–H gel formation, pore refinement, and strengthening of the interfacial transition zone, explaining the observed improvements in compressive, tensile, and flexural strength.

Durability performance improved with increasing calcination temperature due to accelerated calcium hydroxide consumption, reduced portlandite content, and lower pore connectivity, resulting in enhanced resistance to chloride and acid attack. Two-way ANOVA confirmed the statistical significance of these trends, with calcination temperature showing the highest F-values across all properties and significant interaction effects indicating a synergistic influence of temperature and replacement level.

5 Future perspectives

To further substantiate these findings, future research should incorporate quantitative electrochemical measurements—including half-cell potential, Tafel polarization, and electrochemical impedance spectroscopy—to determine corrosion kinetics and passive film stability. Advanced characterization tools such as nanoindentation, BET surface analysis, and 3D micro-computed tomography should be employed to quantify pore connectivity and gel stiffness at the nano–micro scale. Long-term durability testing under marine, sulfate, and carbonation conditions, combined with finite-element corrosion modeling and life-cycle assessment (LCA), will provide comprehensive insight into the service-life extension and environmental benefits of MMT-based concretes. Furthermore, exploring hybrid formulations that couple calcined MMT with other SCMs or natural fibers could open pathways for designing next-generation corrosion-resistant and thermally stable eco-concretes suited for sustainable infrastructure applications.

Data availability statement

The original contributions presented in the study are included in the article/supplementary material, further inquiries can be directed to the corresponding author.

Author contributions

AmH: Conceptualization, Data curation, Formal Analysis, Funding acquisition, Investigation, Methodology, Resources, Software, Writing – original draft, Writing – review and editing. AsH: Project administration, Software, Supervision, Validation, Visualization, Writing – review and editing. RM: Project administration, Software, Supervision, Validation, Writing – review and editing. TA: Conceptualization, Software, Supervision, Validation, Writing – review and editing. FL: Software, Supervision, Validation, Writing – review and editing. YC: Methodology, Project administration, Resources, Software, Supervision, Validation, Visualization, Writing – review and editing.

Funding

The author(s) declared that financial support was received for this work and/or its publication. This research was funded by the HEAT PROJECT of the Mwalimu Julius K. Nyerere University of Agriculture and Technology (MJNUAT). The aims of the HEAT Project are to strengthen the learning environment, ensure greater alignment of priority degree programs to labor market needs, and improve the management of the higher education system.

Conflict of interest

The author(s) declared that this work was conducted in the absence of any commercial or financial relationships that could be construed as a potential conflict of interest.

Generative AI statement

The author(s) declared that generative AI was used in the creation of this manuscript. To write English sentence correctly.

Any alternative text (alt text) provided alongside figures in this article has been generated by Frontiers with the support of artificial intelligence and reasonable efforts have been made to ensure accuracy, including review by the authors wherever possible. If you identify any issues, please contact us.

Publisher's note

References

Abdalla, J. A., Hawileh, R. A., Bahurudeen, A., Jittin, V, Syed Ahmed Kabeer, K., and Thomas, B. (2023). Influence of synthesized nanomaterials in the strength and durability of cementitious composites. *Case Stud. Constr. Mater.* 18, e02197. doi:10.1016/j.cscm.2023.e02197

Ahmed, A. (2024). Assessing the effects of supplementary cementitious materials on concrete properties: a review. *Discov. Civ. Eng.* 1 (1), 145. doi:10.1007/s44290-024-00154-z

Andreola, F., Borghi, A., Pedrazzi, S., Allesina, G., Tartarini, P., Lancellotti, I., et al. (2019). Spent coffee grounds in the production of lightweight clay ceramic aggregates in view of urban and agricultural sustainable development. *Materials* 12 (21), 3581. doi:10.3390/ma12213581

Attah, I. C., Alaneme, G. U., Etim, R. K., Afangideh, C. B., Okon, K. P., and Otu, O. N. (2023). Role of extreme vertex design approach on the mechanical and morphological

behaviour of residual soil composite. *Sci. Rep.* 13 (1), 7933. doi:10.1038/s41598-023-35204-6

Chantal, N. D. (2020). *Influence of addition of metakaolinite and ash oyster shells on Portland cement mortars properties*.

Chung, L. L. P., Wong, Y. C., and Arulrajah, A. (2021). The application of spent coffee grounds and tea wastes as additives in alkali-activated bricks. *Waste Biomass Valorization* 12 (11), 6273–6291. doi:10.1007/s12649-021-01453-7

DuchesneJ., (2021). Alternative supplementary cementitious materials for sustainable concrete structures: a review on characterization and properties. *Waste Biomass Valorization* 12 (3), 1219–1236. doi:10.1007/s12649-020-01068-4

Eliche-Quesada, D., Bonet-Martínez, E., Pérez-Villarejo, L., Castro, E., and Sánchez-Soto, P. J. (2021). Effects of an illite clay substitution on geopolymer synthesis as an alternative to metakaolin. *J. Mater. Civ. Eng.* 33 (5), 04021072. doi:10.1061/(asce)mt.1943-5533.0003690

Fode, T. A., Jande, Y. A. C., and Kivevele, T. (2023). Effects of different supplementary cementitious materials on durability and mechanical properties of cement composite. *Heliyon* 9 (7), e17924. doi:10.1016/j.heliyon.2023.e17924

Fode, T. A., Jande, Y. A. C., and Kivevele, T. (2024a). Effects of raw and different calcined bentonite on durability and mechanical properties of cement composite material. *Case Stud. Constr. Mater.* 20, e03012. doi:10.1016/j.cscm.2024.e03012

Gomes, S. D. C., Nguyen, Q. D., Li, W., and Castel, A. (2024). Effects of mix composition on the mechanical, physical and durability properties of alkali-activated calcined clay/slag concrete cured under ambient condition. *Constr. Build. Mater.* 453, 139064. doi:10.1016/j.conbuildmat.2024.139064

Gu, X., Hu, Z., Hu, Z., Liu, J., Wang, Q., and Nehdif, M. L. (2024). Optimizing calcination temperature to improve the compressive strength of coal gasification slag-based alkali-activated materials by reducing carbon content and adjusting polymerization degree. *Constr. Build. Mater.* 456, 139284. doi:10.1016/j.conbuildmat.2024.139284

Hai, L., and Wang, J. (2024). Experimental study on the heat treatment reaction process of bentonite. *Sci. Rep.* 14 (1), 16649. doi:10.1038/s41598-024-67555-z

Haigh, R., Sandanayake, M., Joseph, P., Arun, M., Yaghoubi, E., Vrcelj, Z., et al. (2024). The thermo-phase change reactivity of textile and cardboard fibres in varied concrete composites. *Sustainability* 16 (8), 3221. doi:10.3390/su16083221

Haque, E., and Armeniades, C. (1986). Montmorillonite polymer concrete: zero-shrinkage and expanding polymer concrete with enhanced strength. *Polym. Eng. & Sci.* 26 (21), 1524–1530. doi:10.1002/pen.760262109

Hepautwa, A. A., and Jande, Y. A. C. (2025). Mechanical, chemical performance, and microstructural behavior of montmorillonite-burnt red soil bricks incorporating coffee ash biochar. *Front. Built Environ.* 11, 1632901. doi:10.3389/fbuil.2025.1632901

Jafari, A., and Sadeghian, P. (2025). Hydrochar from hydrothermal liquefaction of spent coffee grounds for cementitious composites: effects on strength, porosity, microstructure, and carbon footprint. *Constr. Build. Mater.* 475, 141134. doi:10.1016/j.conbuildmat.2025.141134

Kaundal, A., Chaturvedy, G. K., and Pandey, U. K. (2025). Synergistic effects of montmorillonite and rubber aggregates on concrete properties. *Discov. Concr. Cem.* 1 (1), 23. doi:10.1007/s44416-025-00023-7

Khand, S. W., and Nomana, M. (2019). Durability of mortars modified with calcined montmorillonite clay. *Civ. Eng. J.* 5 (7), 1490–1505. doi:10.28991/cej-2019-03091347

Laidani, Z.E.-A., Benabed, B., Abousnina, R., Gueddouda, M. K., and Kadri, E. H. (2020). Experimental investigation on effects of calcined bentonite on fresh, strength and durability properties of sustainable self-compacting concrete. *Constr. Build. Mater.* 230, 117062. doi:10.1016/j.conbuildmat.2019.117062

Langaroudi, M. A. M., and Mohammadi, Y. (2018). Effect of nano-clay on workability, mechanical, and durability properties of self-consolidating concrete containing mineral admixtures. *Constr. Building Materials* 191, 619–634. doi:10.1016/j.conbuildmat.2018.10.044

Latifi, N., Vahedifard, F., Ghazanfari, E., and A. Rashid, A. S. (2018). Sustainable usage of calcium carbide residue for stabilization of clays. *J. Mater. Civ. Eng.* 30 (6), 04018099. doi:10.1061/(asce)mt.1943-5533.0002313

Lei, Z., Li, Z., Zhang, X., and Shi, X. (2021). Durability of CFRP-wrapped concrete in cold regions: a laboratory evaluation of montmorillonite nanoclay-modified siloxane epoxy adhesive. *Constr. Build. Mater.* 290, 123253. doi:10.1016/j.conbuildmat.2021.123253

Liu, M., Hu, Y., Lai, Z., Yan, T., He, X., Wu, J., et al. (2020). Influence of various bentonites on the mechanical properties and impermeability of cement mortars. *Constr. Building Materials* 241, 118015. doi:10.1016/j.conbuildmat.2020.118015

Macías-Párraga, M., Echarri, F. J. T., Alonso-Pandavenes, O., and Garzón-Roca, J. (2025). Improvement of expansive soils: a review focused on applying innovative and sustainable techniques in the Ecuadorian coastal soils. *Appl. Sci.* 15 (15), 8184. doi:10.3390/app15158184

Madirisha, M. M., Dada, O. R., and Ikotun, B. D. (2019). *Materials today sustainability*.

Mahmood, A., Pechočiaková, M., Noman, M. T., Wacławek, S., Gheibi, M., Behzadian, K., et al. (2024). Preparation of green sustainable cement paste mixture based on inorganic additives: an experimental and modelling approach. *Buildings* 14 (7), 1922. doi:10.3390/buildings14071922

Manjunath, B., Ouellet-Plamondon, C. M., Ganesh, A., Das, B., and Bhojaraju, C. (2024). Valorization of coffee cherry waste ash as a sustainable construction material. *J. Build. Eng.* 97, 110796. doi:10.1016/j.jobe.2024.110796

Marangu, J. M. (2020). Physico-chemical properties of Kenyan made calcined clay-limestone cement (LC3). *Case Stud. Constr. Mater.* 12, e00333. doi:10.1016/j.cscm.2020.e00333

Mohammed, A. A., and Nahazanan, H. (2023). Calcined shale and palm oil fuel ash as partial replacements for calcium-based binders to enhance compaction properties of marine clay. *J. Nat. Fibers* 20 (2), 2282057. doi:10.1080/15440478.2023.2282057

Mokhtari, P. (2019). *New low cost and green composite binder for construction*.

Ndahirwa, D., Zmamou, H., Lenormand, H., and Leblanc, N. (2022). The role of supplementary cementitious materials in hydration, durability and shrinkage of cement-based materials, their environmental and economic benefits: a review. *Clean. Mater.* 5, 100123. doi:10.1016/j.clema.2022.100123

Onyelowe, K. C., Aririguzo, J. C., and Ezugwu, C. N. (2019). *Sustainable soils Re-Engineering*. Singapore: Partridge Publishing Singapore.

Pinto, M. S., Marvila, M. T., and de Azevedo, A. R. G. (2023). Chemical treatments for coffee husks: application in mortar for coating and laying blocks. *Buildings* 13 (7), 1678. doi:10.3390/buildings13071678

Qin, Y., Qu, C., Ma, C., and Zhou, L. (2022). One-part alkali-activated materials: state of the art and perspectives. *Polymers* 14 (22), 5046. doi:10.3390/polym14225046

Rashid, S., Raghav, A., Goyal, A., A.B., D. R., and Singh, M. (2024). Biochar as a sustainable additive in cementitious composites: a comprehensive analysis of properties and environmental impact. *Industrial Crops Prod.* 209, 118044. doi:10.1016/j.indcrop.2024.118044

Rashidi, Y., Ashnavar, A., Masoumi, P., Ghaffari, O. b., Khaji, M., and Habibnejad Korayem, A. (2024). Mitigating acid attack-induced deterioration of cement mortar through the application of montmorillonite nanosheets. *Constr. Build. Mater.* 457, 139425. doi:10.1016/j.conbuildmat.2024.139425

Sakir, S., Raman, S. N., Safiuddin, M., Kaish, A. B. M. A., and Mutalib, A. A. (2020). Utilization of by-products and wastes as supplementary cementitious materials in structural mortar for sustainable construction. *Sustainability* 12 (9), 3888. doi:10.3390/su12093888

Saraber, A. (2017). *Fly ash from coal and biomass for use in concrete*.

Shaji, S., and Divya, P. (2024). Sustainable ground improvement of soft clay using eggshell lime and rice husk ash. *Constr. Build. Mater.* 441, 137460. doi:10.1016/j.conbuildmat.2024.137460

Shamsa, M. H., Al-Abdaly, N. M., Jaber, A. A., and Al-Rammahi, A. A. (2022). Effect montmorillonite clay as aggregate in lightweight concrete cement-free. *Periodicals Eng. Nat. Sci.* 10 (2), 147–154. doi:10.21533/pen.v10i2.2894

Wang, N., and Zhang, Z. (2025). Simple preparation of superhydrophobic montmorillonite mortar for enhancing corrosion resistance while maintaining flexural strength. *Constr. Build. Mater.* 500, 144115. doi:10.1016/j.conbuildmat.2025.144115

Wang, Y., Xu, C., and Li, H. (2019). Property and degradation characteristics of concrete prepared with aggregate contained montmorillonite. *J. Wuhan Univ. Technology-Mater. Sci. Ed.* 34 (1), 127–131. doi:10.1007/s11595-019-2025-y

Wu, Z. (2025). Accelerating precuring of autoclaved aerated concrete (AAC) via hybrid alkali-activated pisha sandstone: suppression of montmorillonite swelling and pore structure optimization. *Langmuir*. doi:10.1021/acs.langmuir.5c02888

Yusuf, M. O. (2024). Flyash and coffee silverskin binary blended geopolymer. *Constr. Build. Mater.* 453, 138983. doi:10.1016/j.conbuildmat.2024.138983